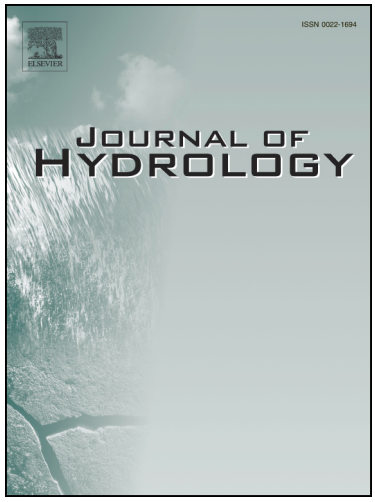

Research papers

Vulnerability Mapping of Coastal Aquifers to Seawater Intrusion: Review, Development and Application

Esmaeel Parizi, Seiyed Mossa Hosseini, Behzad Ataie-Ashtiani, Craig T. Simmons

PII: S0022-1694(18)30970-3
DOI: https://doi.org/10.1016/j.jhydrol.2018.12.021
Reference: HYDROL 23339

To appear in: *Journal of Hydrology*

Received Date: 25 August 2018
Revised Date: 18 December 2018
Accepted Date: 19 December 2018

Please cite this article as: Parizi, E., Hosseini, S.M., Ataie-Ashtiani, B., Simmons, C.T., Vulnerability Mapping of Coastal Aquifers to Seawater Intrusion: Review, Development and Application, *Journal of Hydrology* (2018), doi: https://doi.org/10.1016/j.jhydrol.2018.12.021

Vulnerability Mapping of Coastal Aquifers to Seawater Intrusion: Review, Development and Application

Esmaeel Parizi[a], Seiyed Mossa Hosseini[a,1], Behzad Ataie-Ashtiani[b,c], Craig T. Simmons[c]

[a] Physical Geography Department, University of Tehran, P.O. Box 14155-6465, Tehran, Iran.

[b] Department of Civil Engineering, Sharif University of Technology, P.O. Box 11155-9313, Tehran, Iran

[c] National Centre for Groundwater Research & Training and College of Science & Engineering, Flinders University, GPO Box 2100, Adelaide, South Australia 5001, Australia.

Abstract

In this study, a review of the overlay/index methods served for delineation of vulnerable zones in coastal aquifers affected by SWI is provided. Then, a more realistic presentation of the vulnerability mapping of coastal aquifers to SWI through modified GALDIT index method by incorporating the influential factors on SWI is established. The modifications on GALDIT method including incorporating the seaward hydraulic gradient (i) instead of the height of groundwater level above sea level (L) (so-called GAiDIT), and considering hydraulic gradient (i) as an additional parameter to the GALDIT (so-called GALDIT-i). Three GALDIT, GAiDIT, and GALDIT-i methods were evaluated with data from three coastal confined and phreatic/confined aquifers located in the south of the Caspian Sea, northern Iran. While no highly vulnerable zone was recognized by GALDIT method across three studied aquifers, averagely 43.4% and 50.5% of aquifers area were defined as highly vulnerable zones by GAiDIT and GALDIT-i, respectively. Furthermore, the final vulnerability maps obtained by GALDIT-i and then GAiDIT indicates higher correlation by three groundwater quality indices specific to SWI including f_{sea} (r=0.72 and 0.63) and $\overline{\mathrm{GQI}}$ (r=0.69 and 0.62) and also the distribution of TDS in groundwater (r=0.71 and 0.61) compared with GALDIT (r=0.33, 0.42, and 0.36, respectively). The values of vulnerability index obtained by GALDIT-i and GAiDIT are more strongly correlated with the length of

[1] Corresponding Author. *Email address*: smhosseini@ut.ac.ir (S.M. Hosseini).

SWI into the aquifer (L_x) based on Strack's analytical approach than GALDIT (r=0.52, 0.36, and 0.32, respectively). The results of sensitivity analysis indicated that the hydraulic gradient, height of groundwater level above sea level, aquifer type, and existing status of seawater intrusion has the greatest impact on the groundwater vulnerability across the studied aquifers by GALDIT-i and GAiDIT methods. Results also indicated that serving the influential parameters in GALDIT methods regarding the hydrological and anthropogenic characteristics across the aquifer provide a more realistic characterization of the SWI. This modification leads to an accurate aquifer vulnerability mapping to SWI in aquifers characterized by transient anthropogenic drivers (e.g. pumping) which can be served as a promising tool for decision-making to properly assess and manage risk.

Keywords: Coastal Aquifer; Vulnerability Mapping; Overlay/Index Methods; Seawater Intrusion; Caspian Sea; Modified GALDIT

1. Introduction

Coastal zones (CZs) are among the most important areas around the globe as they are among the most populated and investment regions (Alongi, 1999; Tan et al., 2018). While more than 45% of the world's population (i.e. 2.69×10^9 people in 2018/August) resides within the 100 km landward of coastline, the average population density (APD) of CZs in 2000 (87 people km^{-2}) is nearly four times greater than inland areas (23 people km^{-2}) (Shi and Singh, 2003; Fernandino et al., 2018). The projected APD by UNESCO (2003) in CZs and inland areas are 115 and 44 people km^{-2}, respectively by 2025. CZs comprise <20% of the Earth's surface and the same time is the location of 75% of megacities, with more than 10 million inhabitants. CZs are also a major destination for coastal and maritime tourism. Nearly 80% of all tourism takes place in coastal areas (16.5 million visitors, yearly) with a growth rate of 17% since 1989 (Crossland et al., 2006; Kantamaneni, 2016).

The pressure for further development in CZs requires additional water resources to meet growing demands. In these areas, the demographic pressure and the high level of urbanization cause high water-demand which is increasingly met by groundwater. Furthermore, human activities cause groundwater depletion, triggering seawater intrusion and pollutant dispersion (Parisi et al., 2018). Therefore, the protection of groundwater resources in CZs, as a valuable freshwater resources in these areas, requires cautious measures in particular in arid and semi-arid parts of the world (Costanza et al., 1997; Fuentes et al., 2018).

Seawater intrusion (SWI) is among the main threatening factors for the quantity and quality of groundwater resources in coastal aquifers worldwide. SWI is the landward movement of saline water into coastal aquifers and usually shows seasonal oscillation due to human, and climate-forced factors (Xiao et al., 2016; Baena-Ruiz et al., 2018). Readers are referred to some of the recent review papers in the literature for further information. Werner et al. (2013) have provided a comprehensive review of SWI processes. Ketabchi and Ataie-Ashtiani (2015) reviewed coastal groundwater optimization methods for managing SWI into coastal aquifers. More recently, Ketabchi et al. (2016) reviewed sea-level rise (SLR) impacts on SWI in coastal aquifers.

A type of popular and easy-to-use approach in the study of SWI vulnerability assessments is the indexing method (Klassen and Allen, 2017). Only a few published guidance could be found for rapidly assessing the vulnerability of coastal aquifers to SWI at regional scales (i.e. aquifer scale), particularly in the case of insufficient long-term data (Kallioras et al., 2011; Kura et al., 2014; Luoma et al., 2017; Kazakis et al., 2018).

GALDIT method is an acronym standing for six incorporated indicators including aquifer type (G), hydraulic conductivity of aquifer (A), height of groundwater level above sea level (L), distance from the shoreline (D), some hydrogeochemical evidence about the

presence of SWI such as EC and ion of Cl^- (I), and saturated thickness of aquifer (T) (Chachadi et al., 2007). This method is among the most popular methods for this purpose and it gives relatively accurate results for assessing the vulnerability of large-scale regions with complex in geological settings to SWI (Panagopoulos et al., 2006). GALDIT uses simple indicators with easy-to-collect data that follows also the parsimony principle (Lobo-Ferreira et al., 2007).

A summary of the recent studies that used overlay/index (O/I) methods to delineate the vulnerability of coastal aquifer to SWI is provided in Table 1. Based on the review of the previous studies a variety of O/I methods including original and modified forms of GALDIT (Chachadi and Lobo-Ferreira, 2007), DRASTIC (Allen et al., 1987), SINTACS (Civita and de Maio, 2000), and AVI (Van Stempvoort et al., 1992) have been used for mapping the vulnerability of coastal aquifers to SWI due to both natural and anthropogenic factors. GALDIT method provides quite effective and reasonable results compared to the other afore-mentioned methods due to involving the hydro-dynamic condition of the aquifer, e.g. permeability and groundwater level (Trabelsi et al., 2016). This method provides promising results based on hydrogeochemical indications for the aquifers that are strongly impacted by recharge and exploitation rate, and also SLR due to climate change (Xiao et al., 2016; Luoma et al., 2017) and storm surges (Yang et al., 2013). Whereas the other methods (e.g. DRASTIC and SINTACS) are better suited to consider the vulnerability due to anthropogenic factors (e.g. contamination from the surface), they have no parameters that relate to contamination from SWI (Kallioras et al., 2011; Allouche et al., 2017). Table 1 shows that the most important factors for evaluating the vulnerability of the coastal aquifers to SWI are height of groundwater level above sea level (Pedreira et al., 2015; Recinos et al., 2015; Luoma et al., 2017), hazards due to climate change (i.e. SLR) and overexploitation of aquifers (Lobo Ferreira et al., 2005; Mahesha et al., 2012), and

pumping rate (Docheshmeh-Gorji and Asghari-Moghadam, 2016; Klassen and Allen, 2017). The proficiency of GALDIT among the other O/I methods to map the vulnerability of coastal aquifers to SWI especially in absence of anthropogenic contamination from aquifer surface is revealed from the Table 1 ("Key Findings" column). The drawbacks of I/O methods are the use of qualitative parameters (e.g. Groundwater occurrence in GALDIT), a large amount of data required (especially for GALDIT and SINTACS), and a few vulnerability categorizations (Ivkovic et al., 2013; Luoma et al., 2017). Moreover, they need appropriate indicators for checking the model robustness and verification (Kazakis et al., 2018), and adopting a spatial interpolation method for observed point data across the aquifer (Saidi et al., 2013), and subjectivity in selecting the weights of different attributes (Kallioras et al., 2011). The I/O methods require to serve the most influential factors on SWI according to inherent susceptibility and anthropogenic factors (Werner et al., 2012, Klassen and Allen 2017; Motevalli et al., 2018). Table 1 reveals that the verification of the vulnerability mapped output has been checked by comparison of the results with hydrogeochemical data from groundwater samples, whereas choosing the best verifying indicator is still a challenge (Kazakis et al., 2018).

For the coastal aquifers with overexploitation of groundwater, the seaward hydraulic gradient is the most important variable controlling the seawater toe location and also provides the major source of fresh groundwater discharge to sea (Werner et al., 2012; Ferguson and Gleeson, 2012; Holding and Allen 2015; Comte et al., 2016; Ketabchi et al., 2016). However, the GALDIT method serves the height of groundwater level above sea level as an alternate indicator, but fluctuations of the hydraulic gradient driven by changes in transient recharge/discharge components indicates higher correlation with groundwater salinity especially across the coastline (Anderson and Emanuel, 2010; Gonneea et al., 2013) Awareness of the impact of the hydraulic gradient on SWI, it is not yet included

directly in the O/I method to delineation of vulnerability zones over aquifer scale. This study was motivated by the need to provide a more accurate mapping of the vulnerability of large-scale coastal aquifers to SWI by introducing more influential hydrological factors in an O/I approach. For the first time, it attempts to evaluate the utilization of seaward hydraulic gradient of groundwater flow (i) as an influential indicator in GALDIT method. Accordingly, an alternative quantitative indicator i is served in the original form of GALDIT model, one time instead of height of groundwater level above sea level (L) (so-called GAiDIT), and another time as an additional input parameter (so-called GALDIT-i). The efficiency of three models GALDIT, GAiDIT, and GALDIT-i in generating vulnerability (based on annual-averaged data) and time-evolution hazard (based on seasonal data) mapping are evaluated by the application of the methods on three confined and semi-confined coastal aquifers in the southern coast of the Caspian Sea, Iran. The verification of the final vulnerability maps produced by three methods over three studied aquifers was carried out using three groundwater chemical indicators of fresh and seawater and also the length of the seawater intrusion at the point beneath the shoreline into the aquifer section based on Strack (1976) analytical solution. The meaningfulness of the incorporated parameters into three models (GALDIT, GAiDIt, and GALDIT-i) for vulnerability mapping of aquifers to SWI are also discussed.

2. Materials and Methods

2.1. GALDIT Approach

GALDIT is an overlay/index method to assess the spatial intrinsic vulnerability of coastal aquifer systems to seawater intrusion developed based on a parametric system with rating scores and weights for six most important factors controlling seawater intrusion (Chachadi and Lobo-Ferreira, 2001). A summary of parameter weights, rates, and ranges used in GALDIT method are given in Table 2. Originally, Chachadi and Lobo-Ferreira (2001)

suggested the ratio of $Cl^-/[HCO_3^- + CO_3^{2-}]$ for rating the impact status of the existing SWI. Later, Dörfliger et al. (2011) and Luoma et al. (2017) added EC values and Cl concentration of groundwater from wells along the coastline as alternative indices of existing SWI and reclassified the related rates.

In each grid cell, each parameter was rated as R_i based on its vulnerability to seawater intrusion being 2.5 (lowest vulnerability), 5, 7.5, and 10 (highest vulnerability). These assigned rating parameters were multiplied by the weight strings (W_i) being 1 (lowest significant parameter) to 4 (highest significant parameter) to obtain final vulnerability index in each grid (Chachadi, 2005):

$$\text{GALDIT} = \frac{\sum_{i=1}^{6} W_i \times R_i}{\sum_{i=1}^{6} W_i} \quad (1)$$

The GALDIT index categorized in three classes: low (<5), moderate (5 to 7.5), and high vulnerability (>10).

2.2. Modifications to GALDIT

In this study, two modifications are made on the input parameters of the GALDIT model: 1) replacing the height of groundwater level above sea level (L) with the seaward hydraulic gradient ($i = dh/dx$) (i.e. GAiDIT method), and 2) serving the parameter i as an additional parameter into the GALDIT model (i.e. GALDIT-i method). Hydraulic gradient, a vector having both a direction and magnitude, represents the slope of the water table or potentiometric surface and is the driving force for groundwater flow within an aquifer (EPA 2014). Previous studies (e.g. Loaiciga et al., 2012; Ataie-Ashtiani et al., 2013, Ketabchi et al., 2016) demonstrated through the analytical and numerical models that the dominant factors controlling the seawater toe location are the magnitudes of fresh groundwater discharge to sea (parameter q' in Fig. 1), recharge rate, SLR, landward hydraulic head, aquifer thickness, density difference ratio of freshwater and seawater, and

slope of aquifer bed, respectively. In this study, hydraulic gradient (i) at each point is estimated by $(h_{SW} - h_{LW})/x$, where, h_{SW} $[L]$ and h_{LW} $[L]$ is seaward and landward hydraulic head or potentiometric surface, respectively, and x $[L]$ is aquifer length. Landward or seaward direction of i is defined by its negative and positive sign, respectively. The hydraulic gradient inflexion point (i.e. the interface between landward and seaward direction of i) is a key factor in determining the degree of SWI (Fetter, 2001). Spatiotemporal changes in i can be due to changes in aquifer recharge from the ground surface, pumping rates of nearby water supply wells, or changes in nearby surface water elevations and also transmissivity of the aquifer (Ketabchi et al., 2016). In this study, the seaward values of i (i.e. positive values) are rated and embedded in the GALDIT model instead of parameter L. Based on studies of Fetter (2001) and thereafter, Werner (2017), seaward freshwater flow causing passive SWI class which is frequently observed in the confined aquifers (as also observed in the studied aquifers), whereas both seaward and landward freshwater flow causing both active and passive SWI classes. The modifications on the input parameters of the GALDIT method are also shown schematically in Fig. 2. Therefore, based on improvements on the GALDIT for producing the vulnerability mapping of a coastal aquifer to SWI, the GAiDIT uses six input parameters including groundwater occurrence (G), aquifer hydraulic conductivity (A), seaward hydraulic gradient of freshwater (i), distance from the shoreline (D), impact of the existing status of seawater intrusion (I), and aquifer saturated thickness (T) as input parameters. Whereas the GALDIT-i model uses seven parameters G, A, L, D, I, T, and i as input. The vulnerability ratings used for the parameters G, A, L, D, I, and T are the same as the GALDIT method and are presented in Table 1. The vulnerability ratings adopted in this study for the parameter i are presented in Table 2.

The inputs, processes, and steps required to be followed to apply two indices of GALDIT, GAiDIT, and GALDIT-i for vulnerability mapping of coastal aquifers to SWI are schematized in Fig. 2. The procedure includes: collecting information, maps and raw data (e.g. well logs, hydraulic and hydrodynamic parameters of aquifers, groundwater and seawater quality); implementing interpolation/processes in GIS environment required to establish the distributed parameters over aquifer in form of raster maps; rating the parameters according to Table 1; producing the vulnerability maps of coastal aquifers by calculating the indices of GALDIT, GAiDIT, and GALDIT-i (integrating the weighted layers of considered parameters in each method); accuracy assessment of produced vulnerability maps by comparing the spatial distribution of vulnerability indices values, some important factors of SWI presence developed based on groundwater quality parameters including total dissolved solids (TDS), groundwater quality index (GQI), fraction of seawater (f_{sea}), and the length of the seawater intrusion into the aquifer section (L_x); and sensitivity analysis of all incorporated parameters in two vulnerability indices.

2.3. Study Area

To compare and evaluate the GALDIT, GAiDIT, and GALDIT-i approaches in the vulnerability mapping of the coastal aquifer to SWI, three coastal aquifers Astaneh-Koochesfahan (As-Ko), Fomanat, and Lahijan-Chaboksar (La-Ch) along the southern coast of Caspian Sea, at the northern part of Iran are considered, due to the availability of enough required data. Fig. 3 shows the location of three studied aquifers and exploration and piezometric wells. The aquifers are in south Caspian Sea basin and known as a part of the Alborz tectonical range in Alpine fold belt. Due to the influence of Mediterranean air masses, three plains receive high rainfall (more than 1000 mm, annually). According to geologic cross section of three aquifers shown in Fig. 4, Fomanat aquifer (with area of 2027 km^2) is a fully confined aquifer, whereas As-Ko (with area of 2027 km^2) and La-Ch

(with area of 2027 km^2) are confined/ phreatic aquifers, respectively (GRWA 2015, report No. 8353/111). Table 3 summarizes the hydrogeology and hydrogeochemistry characteristics of the studied aquifers.

Based on the geology map of Alborz Zone at scale of 1:100,000 provided by Geological Survey and Mineral Explorations of Iran (GAI, 1997), three aquifers covered by late Pleistocene and Holocene (Quaternary age) well-sorted deposits consisting of: deltaic alluviums (29.5% in La-ch, 78.8% in As-Ko, and 18.7% in Fomanat), marine deposits (48.8% in La-ch, 4.3% in As-Ko, and 81.3% in Fomanat), beach deposits (21.7% in La-ch, 15.3% in As-Ko) and a small coverage of fluvial deposits (1.6% in As-Ko).

According to Stocklin (1968) the three plains are located in a tectonically active area. The surface slopes of three plains are less than 2% which are categorized as flat plains (Davis, 1987). The groundwater level in three aquifers near the Caspian Sea (north parts) is below the MSL (mean Caspian Sea level is -26.5 m below MSL) (see also Table 3). According to monitoring networks of piezometers, the groundwater level of three aquifers indicates insignificant decline (less than 0.1 m, annually) during the last 20 years (1994-2013). The groundwater flow in three aquifers has a general direction from the south to north (i.e. the Caspian Sea), northeast and northwest based on previous tracer tests (GRWA, 2015). In the studied aquifers, groundwater quality sampling was conducted by Guilan regional water authority (GWRA) during 2002 to 2011 through 23 (in La-Ch), 44 (in Fomanat), and 19 (in As-Ko) piezometric wells.

The Southern Caspian Sea is characterized by salinities of nearly 8.0±0.5 g/L (in the west) to 13.0±0.5 g/L (in the east) which increases from the surface to the bottom of the sea (Leroy et al., 2007). Even with this low salinity boundary, the coastal aquifers are faced with SWI due to the presence of relict connate seawater within the permeable Holocene sediments of the semi-confined aquifers (Kosarev and Yablonskaya, 1994). Additionally, the freshwater demands for agricultural and domestic water are mostly supplied by

groundwater exploitation of the coastal aquifers, because of accessibility (low depth of groundwater as shown in Table 3) and high storage capacity of the groundwater in these alluvial aquifers (Gholami et al., 2010).

2.4. Verification of Vulnerability Maps

To avoid flawed decisions and subjective environmental assessments on the final vulnerability maps, verification of the produced vulnerability indices by the GALDIT, GAiDIT, and GALDIT-i methods with the measured data is necessary. Three considered aquifers have long-term hydrogeochemical data and this allows to define different indices. According to Fig. 2, four indices including spatial distribution of TDS in groundwater, fraction of seawater (f_{sea}) into groundwater, groundwater quality indices ($\overline{\mathrm{GQI}}$), and the length of the seawater intrusion at the into the aquifer section (L_x) serve to verify the produced vulnerability maps. The following describes how the indices of f_{sea}, $\overline{\mathrm{GQI}}$, and L_x are developed.

1) Fraction of seawater (f_{sea}): since, chloride (Cl^-) and sodium (Na) make up nearly 85% of the total ionic composition of seawater, increasing Cl^- concentration within the aquifer can be used as an indicator for SWI (Richter and Kreitler, 1993). Fraction of seawater (f_{sea}) introduced by Appelo and Postma (2005) is used as a verification parameter to assess the produced vulnerability maps:

$$f_{sea} = \frac{\mathrm{Cl}_i - \mathrm{Cl}_{\mathrm{fw}}}{\mathrm{Cl}_{\mathrm{sw}} - \mathrm{Cl}_{\mathrm{fw}}} \qquad (2)$$

where Cl_i is the concentration of Cl^- in groundwater at i^{th} location (meq/l), $\mathrm{Cl}_{\mathrm{fw}}$ and $\mathrm{Cl}_{\mathrm{sw}}$ are the concentration of Cl^- in freshwater and seawater (meq/l), respectively. The f_{sea} values ranging from 0 to 1 denotes to freshwater and seawater, respectively. Fraction of seawater index (f_{sea}) fails to identify hydrogeochemical reactions associated with SWI that can mostly affect the ionic composition of groundwater in coastal aquifers (Appelo, 1987).

These reactions including cation exchanges, dolomitization, and sulfate reduction which produce Ca^{2+}, S^{2-}, and HCO_3^- ions (Panteleit et al., 2011).

2) Groundwater quality indices ($\overline{GQI}$): Alkaline groundwater in coastal aquifers may have a high concentration of Cl^- due to SWI, but be less saline. Therefore, besides electrical conductivity (EC) of groundwater in the aquifers as a simple indicator of salinity, two groundwater quality indices GQI_{mix} and GQI_{dom} developed by Tomaszkiewicz et al. (2014) are used to aggregate hydrochemical data of different ions:

$$GQI_{mix} = \left[\frac{Ca^{2+} + Mg^{2+}}{TC} + \frac{HCO_3^-}{TA}\right] \times 50 \quad (3)$$

$$GQI_{dom} = \left[\frac{Na^{+} + K^{+}}{TC} + \frac{HCO_3^-}{TA}\right] \times 50 \quad (4)$$

where TC and TA are concentration of total cations and anions in groundwater, respectively. The concentrations of ions in Eqs. 3 and 4 are meq/l. The indices GQI_{mix} and GQI_{dom} range from 0 (representing saline water and $Ca-Cl$ water type, respectively) to 100 (representing fresh water and $NaHCO_3$ water type, respectively).

To group the essential character of groundwater quality into different domains, the calculated values of GQI_{mix} and GQI_{dom} are presented on the diamond field of Piper diagram (Piper, 1944; Singhal and Gupta, 2010) (Fig. 5). The domains resulted including: I, II, III, IV, V, VI, representing water type of $CaHCO_3$, NaCl, mixed $CaNaHCO_3$, mixed CaMgCl, CaCl, and $NaHCO_3$, respectively (Sarath Prasanth et al., 2012). Coupling the Piper diagram and groundwater quality indices (GQI_{mix} and GQI_{dom}) is a widely and simple method to identify the SWI and hydrogeochemical pathways in the coastal aquifers based on major ions relevant in groundwater (Appelo and Postma, 2005).

3) The length of the seawater intrusion into the aquifer (L_x): when the steady-state salinity distribution occurs after the inland movement of saline water/freshwater interface, the

parameter L_x offers an insight into the propensity for SWI and understanding the vulnerability of a coastal environment (Zhou 2011, Werner et al., 2012). Moreover, L_x allows to consider the instability in interface position through future stresses (e.g. change in recharge due to climate change or over extraction by the pumping) (Nofal et al., 2015). The parameter L_x can be derived from the steady-state sharp-interface equations of Strack (1976, 1989). For an unconfined and confined coastal aquifer experiencing distributed recharge and with the conditions that shown in Fig. 1, the freshwater groundwater discharge to the sea, $q'[L^2T^{-1}]$ based on the method developed by Strack (1976, 1989) is as follows:

$$q' = \begin{cases} \frac{K}{2x}\left[\left(h_{f_x} + z_0\right)^2 - (\delta+1)z_0^2\right] + \frac{W_{net}\,x}{2} & ; \quad \text{for unconfined aquifer} \\ \frac{Kh_0}{x}\left[h_{f_x} - \delta\left(h_{f_x} - \frac{h_0}{2}\right)\right] + \frac{W_{net}\,x}{2} & ; \quad \text{for confined aquifer} \end{cases} \tag{5}$$

where h_{f_x} $[L]$ is the fresh-water hydraulic head above the MSL in each distance x $[L]$ from shore-line; h_0 $[L]$ is confined aquifer thickness respect to base of aquifer; W_{net} $[L\,T^{-1}]$ is net recharge to aquifer after subtracting all losses including evapotranspiration, storage in vadose zone, pumping, and leakage (for confined aquifer) which maybe a negative or positive value; K $[L\,T^{-1}]$ is saturated hydraulic conductivity of aquifer formations; ρ_s $[M\,L^{-3}]$ and ρ_f $[M\,L^{-3}]$ are sea-water and freshwater density, respectively; δ $[-]$ is density difference ratio of the seawater and freshwater terms as $\delta = (\rho_s - \rho_f)/\rho_f$; and z_0 $[L]$ is depth to horizontal base of the aquifer below the MSL. For brevity, we refer the reader to Werner et al. (2012) and Ataie-Ashtiani et al. (2013b) for further details of the method. The Eq. 5 is valid for the landward of interface ($x > L_T$). Using the Eq. 5 negative values is obtained for the q' under passive SWI condition (Badaruddin et al., 2015). According to Fetter (1973, 2001), passive SWI condition referring to inland movements of seawater in areas where fresh groundwater flows towards the coastline. Awareness of h_{f_x}

at different location x (from piezometric monitoring network), ρ_s, ρ_f, z_0, h_0, K, and W_{net}, the value of q' can be obtained from the Eq. 5.

Replacing the Ghyben-Herzberg equation as $h_{f_x} = \delta z_x$ (Ghyben, 1889; Herzberg, 1901) in the Eq. 5, the length of the seawater intrusion at the point beneath the shoreline into the aquifer section (L_x $[L]$) under condition shown in Fig. 1 is obtained as:

$$L_x = \begin{cases} \frac{q\prime}{W_{net}} + \xi\sqrt{\left(\frac{q\prime}{W_{net}}\right)^2 - \frac{K}{W_{net}}[(\delta z_x + z_0)^2 - (\delta+1)z_0{}^2]} \text{ ; for unconfined aquifer} \\ \frac{q\prime}{W_{net}} + \xi\sqrt{\left(\frac{q\prime}{W_{net}}\right)^2 - \frac{2Kh_0}{W_{net}} - \delta z_x + \delta\left(z_0 - \frac{h_0}{2}\right)} \text{ ; for confined aquifer} \end{cases} \quad (6-a)$$

where

$$\xi = \begin{cases} +1 & \text{if} \quad W_{net} < 0 \\ -1 & \text{if} \quad W_{net} > 0 \end{cases} \quad (6-b)$$

The length of the seawater intrusion wedge (L_T) can be obtained from the Eq. 6 by replacing $z_x = z_0$ at the wedge toe:

$$L_T = \begin{cases} \frac{q'}{W_{net}} + \xi\sqrt{\left(\frac{q'}{W_{net}}\right)^2 - \frac{K}{W_{net}}\delta(1+\delta)z_0{}^2} \; ; & \text{for unconfined aquifer} \\ \frac{q'}{W_{net}} + \xi\sqrt{\left(\frac{q'}{W_{net}}\right)^2 - \frac{K\delta h_0^2}{W_{net}}} \; ; & \text{for confined aquifer} \end{cases} \quad (7)$$

Equation 7 is also consistent with the one derived by Werner et al. (2012), Ataie-Ashtiani et al. (2013b) and Ketabchi et al. (2016). Another advantages of using the parameter L_x in assessment of SWI vulnerability is its dependency to influenced parameters of q', W_{net}, δ, K, z_0, and h_0 to delineate the length of the seawater intrusion into the aquifer which may differ for the points with same distance from the shoreline.

It is noteworthy that in long-screened pumping wells and especially those left un-pumped for a long time, contribution of intraborehole flow regime (IFR) due to vertical hydraulic gradient across screen or open intervals around the substantially alter the chemical mixture of local groundwater around the well (Poulsen et al., 2018). This may introducing

erroneous and misleading results for better understanding and construction of the SWI process and location (McMillan et al., 2014). Water sampling from these wells should be taken after an enough pumping period to sure fully purging of IFR so the well yields native groundwater (Cook et al. 2017).

Before verifying the produced vulnerability maps by GALDIT, GAiDIT, and GALDIT-i with indices of TDS, f_{sea}, $\overline{\mathrm{GQI}}$, and length of SWI into the aquifer (L_x), independence of these data should be tested. Multicollinearity statistics (MCT) including variance inflation factor (VIF) and tolerance value of determination coefficient (TV) (Belsley et al., 1980) are conducted in Statistical Package for the Social Sciences software, SPSS, version 16 (SPSS, Inc., 2001) to test the independence of final vulnerability scores and corresponding values of TDS, f_{sea}, $\overline{\mathrm{GQI}}$, and L_x in three studied aquifers.

2.5. Preparation of Vulnerability Indicators

Groundwater occurrence (aquifer type) (G): The extent of SWI depends on the type of the aquifer in the study area (i.e. confined, unconfined, leaky confined, and bounded) (Table 2). A confined aquifer is more prone to SWI due to the instantaneous release of water to wells during pumping and also the larger cone of depression further adds the vulnerability. According to Chachadi et al. (2007), if multiple aquifers are present in an area (i.e. aquifers As-Ko and La-Ch as shown in Table 3), the highest rating (score 10) can be adopted. Therefore, the assigned rate for parameter G over three studied aquifers in the three methods of GALDIT, GAiDIT, and GALDIT-i is 10. Well logs information were collected from the GWRA (2014) and digitized to prepare the geological map of three studied aquifers by RockWorks visualization software (Rockware, Inc., 2010) (see also Fig. 4). The ratings adopted for the parameter G were described in Table 1.

Aquifer hydraulic conductivity (A): Hydraulic conductivity of an aquifer represents the ability of water transmission through aquifer formations (Allen et al., 1987) can influence

366 the magnitude of SWI. The grid map of hydraulic conductivity is prepared based on point
367 data of pumping test (transmissivity) and saturated thickness of aquifer and interpolating
368 over the aquifer area. In the rating of parameter K, the effect of hydraulic barriers like
369 impervious dikes parallel to the coast and clay layers which may act as walls to SWI
370 should be considered (Chachadi and Lobo-Ferreira, 2001). The average values of hydraulic
371 conductivity varying from 0.1 to 16.75 m/day for aquifer La-Ch, 0.2 to 64.1 m/day for
372 aquifer Fomanat, and 0.3 to 96.0 m/day for aquifer As-Ko. Assigned rates to the feature
373 A for three aquifers are shown in Figs 6(a-c). Three methods of GALDIT, GAiDIT, and
374 GALDIT-i use identical rating values for the parameter A.

375 *Height of groundwater level above sea level* (L): In the GALDIT and GALDIT-i
376 approaches, the level of ground-water with respect to mean sea elevation (MSL) is the
377 most important factor of the SWI evolution in a coastal aquifer (Chachadi et al., 2007). The
378 annual-averaged values of parameter L (during year 2013) varying from 4.0 to 136.0 m for
379 aquifer Fomanat, 0.2 to 90 m for aquifer La-Ch, and 4.8 to 73.1 m for aquifer As-Ko.
380 Assigned rates to the feature L for three aquifers are shown in Figs 6(d-f).

381 In the GAiDIT and GALDIT-i approaches, the hydraulic gradient (i) is used instead of the
382 parameter height of groundwater level above sea level based on aforementioned reasons.
383 The direction of parameter i (Figs. 6-p to 6-r) are valid for both recharge and highly
384 withdraw seasons (i.e. December and August, respectively). Grid maps of L and i for three
385 studied aquifers were produced by interpolating the average groundwater level data
386 collected in year 2013 from the observation wells by GWRA (2014). The hydraulic
387 gradient through three aquifers was oriented in a north and northeast direction toward the
388 Caspian Sea and the irrigation wells with an average magnitude varying from 0.1 to 2.7
389 percent for aquifer La-Ch, 0.1 to 1.8 percent for aquifer Fomanat, and 0.1 to 2.3 percent for
390 aquifer As-Ko, which is not significantly different in irrigation and non-pumping

conditions. In the aquifers AS-Ko and Fomanat, some hydraulic gradient inflexion points can be observed near to shoreline. However, mapping the i values allowed for a rapid evaluation and forecasting of the SWI class especially in the transient conditions where seawater movements had not yet provided a distinct indication of the final steady-state salinity distribution (Morgan et al., 2015). Figures 6(p-r) show the rated values assigned for the parameter i over the three aquifers.

Distance from the shore line (D): The impact of SWI reduces as it moves inland (Chachadi et al., 2007). Table 2 provides general guidelines for rating of the parameter D used in three approaches of GALDIT, GAiDIT, and GALDIT-i. The rated values assigned for the parameter D is shown in Fig. 6(g-i).

Impact of the existing status of seawater intrusion (I): Since ions of Cl^- and HCO_3^- dominates in the seawater and natural groundwater, respectively, Chachadi and Lobo-Ferreira (2001) recommended the concentration of Cl^-, ratio of $Cl^-/[HCO_3^- + CO_3^{2-}]$, and electrical conductivity (EC) can be used to assign the rating of the parameter I in GALDIT approach. The rating adopted in Table 2 for the parameter I is also used in GAiDIT and GALDIT-i methods to assess SWI in a coastal aquifer. The concentration of Cl^- (annual-averaged of 2013) varying averagely from 0.2 to 8.34 mg/l for Fomanat, 1.0 to 7.0 mg/l for As-Ko, and 0.12 to 8.9 for La-Ch. The ratio of $Cl^-/[HCO_3^- + CO_3^{2-}]$ varying averagely from 0.05 to 1.14, 0.04 to 2.5, and 0.01 to 1.53, for aquifer Fomanat, La-Ch, and As-Ko, respectively. Figures 6(j-l) shows the assigned rates to the parameter I over three studied aquifers which is identically used in GALDIT, GAiDIT, and GALDIT-i. Beforehand, the presence of the seawater in the groundwater of coastal aquifers was described by Piper diagram in the confluence of two quality indices of GQI_{mix} and GQI_{dom} (Fig. 5).

Aquifer saturated thickness (T): Extension and magnitude of SWI in the coastal aquifers is directly related to the saturated thickness of the aquifer (Chachadi et al., 2007). Average

values of the parameter T vary from 47 to 182 m for As-Ko, 29 to 206 m for Fomanat, and 38 to 147 m for La-Ch. Table 2 supplements the ratings for various ranges of T. Three methods of GALDIT, GAiDIT, and GALDIT-i use identical rates for the parameter T as shown in Figs. 6(m-o).

Mapping of the groundwater intrinsic vulnerability index through GALDIT, GAiDIT, and GALDIT-i methods for three studied aquifers was performed using the ArcMap program version 10.1. Each parameter was converted to a grid map with grid cell size of 10 × 10 m. The rating and weighting were performed for each parameter using the map overlay analytical function in the Spatial Analyst module of the ArcMap program. Accumulation of weighted parameter maps in the three GALDIT, GAiDIT, and GALDIT-i approaches produce the final vulnerability map.

3. Results and Discussions

A selection of parameter combinations derived from three studied aquifers based on the latest available hydrogeological data (annual-averaged data of year 2013) is given in Tables 4 and 5. Some of these parameters (e.g. A, K, and ρ_s) are inferred from the study area and therefore are only rough approximations of the general conditions of the studied aquifers. The parameters q' and L_T are computed from the Eqs. 6 and 7, respectively. The values obtained for L_T are consistent with the ones reported by Golshan et al. (2018) which determined the location of SWI wedge by vertical resistivity sounding and electromagnetic survey in the east of studied region between 350 to 800 m from the shoreline. Awareness of the parameter values for each aquifer given in Tables 4 and 5, the corresponding values of L_x at each point x can be computed using the Eq. 6.

The diamond field of the Piper diagram and the values of $\mathrm{GQI_{mix}}$ and $\mathrm{GQI_{dom}}$ (Eqs. 3 and 4) developed for the latest observed chemical quality data of groundwater (year 2013) in

two months of November and August (as the least and highest withdraw month, respectively) for three studied aquifers are shown in Fig. 5. The groundwater of Fomanat and La-Ch for two months (November and August) is classified in three zones of I, IV, and V, representing the water type $NaHCO_3$, mixed CaMgCl, and CaCl, respectively. While groundwater of As-Ko for both months November and August classified in two zones of I and IV, indicating water type $NaHCO_3$ and mixed CaMgCl, respectively. The range of calculated values of GQI_{mix} and GQI_{dom} (Fig. 5) indicate higher values for the August in comparison to December for three studied aquifers. The obtained values of GQI_{mix} and GQI_{dom} and the domains of groundwater type indicate the presence of saline groundwater (for three aquifers), seawater (especially for Fomanat in August), cation exchange and sulfate reduction (for three aquifers), and dolomitization and dedolomitization which produces secondary saline groundwater (in August for Fomanat and La-Ch). The right trend of hydrogeochemical data in August compared to December is evidence of mixing of fresh and saline water in the three aquifers. The results obtained indicate the SWI for Fomanat and La-Ch aquifers (higher values of GQI_{mix} and GQI_{dom}), while mixing fresh and saline water occurs in As-Ko. Moreover, the fresh groundwater (data in domain I) is not frequently observed in both months of August and December in As-Ko.

The produced vulnerability maps of three studied aquifers generated by the GALDIT, GAiDIT, and GALDIT-i methods are given in Fig. 7 (a-i). The moderate vulnerable zone obtained by the GALDIT method is limited to a thin length of the aquifers beneath the shore (except a small area in the east of Fomanat aquifer), whereas no high vulnerable zone is delineated by this method. High vulnerable zone with a considerable area of three studied aquifers was defined by both GAiDIT and GALDIT-i methods. The vulnerability maps produced by GAiDIT and GALDIT-i methods exhibit similar patterns and showed small differences in the finer detail. Two modified models define some parts of aquifers

(e.g. west part of Fomanat and southeast of La-Ch) as low vulnerable zone despite their vicinity to the sea (Fig. 7), due to dominant influences of i and hydraulic conductivity (indicator A) on the final map.

The classified vulnerability indexes obtained by the three models (GALDIT, GAiDIT, and GALDIT-i) are given in Table 6. Each category reflects an aquifer's inherent capacity for SWI. The map area with a high GAiDIT vulnerability index covers 58.1%, 49.0%, and 44.3% of the aquifer area La-Ch, As-Ko, and Fomanat, respectively. Whereas, Whereas, the high vulnerable area defined by GALDIT-i for aquifers La-Ch, As-Ko, and Fomanat are 43.5%, 49.8%, and 30.8%, respectively. None of three aquifers has high vulnerability areas according to GALDIT method. The GALDIT model generates low vulnerable areas much greater than both GAiDIT and GALDIT-i models. The areas of moderate and high vulnerability classes obtained by GALDIT are much smaller than two other models. The maximum and minimum high vulnerable zone is obtained for the aquifer La-Ch (58.1%) by GAiDIT model. While no low vulnerable zone is obtained by the GALDIT-i method for aquifer AS-Ko (0.3%), 78.4% and 19.7% of this aquifer area are identified as low vulnerable zones by the GALDIT and GAiDIT models, respectively. Generally, the results of Table 6 indicates the GALDIT method tends to generate low and moderate vulnerable areas.

Results of independency tests in significant level of α=0.05 indicate that all values of VIF and TV for intercomparison of vulnerability scores (as dependent variable) and four indices (as independent variable) are equal to 1.0. This means that the vulnerability scores obtained by three methods statistically are independent of the indices TDS, f_{sea}, $\overline{\mathrm{GQI}}$, and L_x.

The vulnerability maps produced by the GALDIT-i and GAiDIT for three studied aquifers have more consistency with the maps of TDS concentrations, and distributions of quality

indices of f_{sea}, $\overline{\text{GQI}}$, and length of SWI into aquifer (L_x) as shown in Fig. 8. In addition, the Pearson's correlation coefficient (r) between the vulnerability index values produced by the three models and corresponding TDS, f_{sea}, $\overline{\text{GQI}}$, and L_x values are computed and given in Table 7. Although, all correlation coefficients listed in Table 7 are significant at significant level α=0.05, but the GALDIT-i followed by GAiDIT outperforms the GALDIT with an average modification respectively equal to 48.2% and 19.9% (for As-Ko), 77.9% and 59.0% (for La-Ch), and 127.3% and 93.1% (for Fomanat) in r value. On average, the maximum correlation of GALDIT-i and GAiDIT vulnerability indexes in three aquifers is obtained with the f_{sea} (r =0.72) and $\overline{\text{GQI}}$ (r=0.63), respectively. Whereas, the maximum correlation of GALDIT index is obtained, on average, with the $\overline{\text{GQI}}$ equal to 0.42. The difference between the final vulnerability maps produces by GALDIT, GAiDIT, and GALDIT-i methods is believed to be related to the modifications implemented in the incorporated indices (i.e. parameter i) which shows better presentation of transient recharge/discharge components of groundwater at local spatio-temporal scale.

The vulnerability maps produced by the three methods are based on annual-averaged data, but utilization of the time-evolution parameters in these approaches (i.e. parameters L and i) may lead to seasonal hazard maps of aquifer to SWI. Figure 9 shows the vulnerability maps produced by the GALDIT, GAiDIT, and GALDIT-i methods over La-Ch aquifer (for instance) based on corresponding data of dry (September) and wet (March) seasons. Results shown in Fig. 9 (b and d) reveals the difference of aquifer vulnerability area produced by the GAiDIT for dry (15.0% low vul., 39.0% moderate vul., and 46.0 high vul.) and wet (20.0% low vul., 48.5% moderate vul., and 31.5% high vul.) seasons. The corresponding areas to different vulnerability classes produced by the GALDIT-i are 8.3% (low vul.), 30.0% (moderate vul.), and 61.0% (high vul.) in dry season, and 9.7% (low vul.), 44.0% (moderate vul.), and 45.0% (high vul.) in wet season. While the seasonal

hazard map of La-Ch aquifer produced by the GALDIT method for the dry (93.8% low vul., and 6.2% moderate vul.) and wet period (94.3% low vul., and 5.7% moderate vul.) has not substantial difference as shown in Fig. 9 (a and c). The difference between the vulnerability maps in dry and wet season (especially in a high vulnerable area) caused by anthropogenic effect (i.e. pumping for agricultural demands) in three studied aquifers.

Sensitivity analysis was performed to examine the contribution degree of six indicators to the final vulnerability maps through GALDIT, GAiDIT, and GALDIT-i methods using the equation (8) (Li and Merchant, 2013):

$$\mathrm{PV} = \frac{\mathrm{Vul_j} - \mathrm{Vul_0}}{\mathrm{Vul_0}} \times 100 \qquad (8)$$

where PV is the percentage of variation in the vulnerability index (%), $\mathrm{Vul_j}$ is the vulnerability score affected by changes in specific indicator j, and $\mathrm{Vul_0}$ is the vulnerability score for the initial condition (without changes in the values of indicators). For instance, the PV values for the GALDIT, GAiDIT, and GALDIT-i vulnerability indices respect to 10% of increase in the scores of influential indicators are calculated for three studied aquifers and shown in Table 8. Results indicate the predominant influence of indicator G (i.e. aquifer type) on the both GALDIT and GAiDIT vulnerability index adopted for three aquifers. After the aquifer type (G), hydraulic conductivity (indicator A) and hydraulic gradient (i) have the greatest impact on GAiDIT index. While in the GALDIT index, the hydraulic conductivity (A) and distance from the shoreline (D) have the greatest influence after the indicator G. The impact of the existing status of seawater intrusion (indicator I) has the minimum influence on both vulnerability indices of GALDIT and GAiDIT adopted for three studied aquifers. However, according to the guideline given in Table 1, the weights of indicator I is equal to G. This is related to hydrogeochemical properties of groundwater in the studied aquifers (particularly Cl^- concentration), since duplicating the weight of indicator I does not significantly change the final vulnerability index through

both methods. aquifers hydraulic gradient, recharge rate, freshwater flux to the sea, the contrast in freshwater and seawater density, saturated thickness of the aquifer, and hydraulic conductivity of the aquifer materials could be considered as dominant factors causing SWI.

4. Conclusion

In this study, a tabulated review of the vulnerability studies of the coastal aquifers based on overlay/index methods was presented. These methods require to identify the most influential factors on SWI according to inherent susceptibility and anthropogenic factors. In this regard, two modifications were proposed on the input parameters of GALDIT method: with replacing the height of groundwater level above sea level (parameter L) by seaward hydraulic gradient of freshwater (parameter i) (GAiDIT method), and by considering the parameter i as an additional input parameter of GALDIT (GALDIT-i method). Three methods of GALDIT, GAiDIT, and GALDIT-i were evaluated in the three coastal aquifers to delineate the groundwater vulnerability zones to SWI. Three groundwater chemical indices specified for SWI including fraction of seawater (f_{sea}), groundwater quality index (GQI), the concentration of TDS, and length of seawater intrusion (L_x) estimated by Strack's analytical solution were used for validation of two vulnerability indices. Results indicated that modifications implemented on the GALDIT method (especially GALDIT-i) have significantly increased the correlation of final vulnerability scores with four indices of f_{sea}, GQI, TDS, and L_x. Therefore, the suggested methods (GALDIT-i and GAiDIT) provide a better representative of the vulnerable zones of the studied aquifers. The proposed models could potentially be used as a more accurate groundwater vulnerability assessment that is a helpful and excellent decision-making tool for groundwater management and risk assessment of aquifer subject to SWI.

564 The results of sensitivity analysis indicated that the hydraulic gradient (parameter i) and
565 groundwater height above sea level (parameter L) has the great impact on the groundwater
566 vulnerability across the studied aquifers by GAiDIT and GALDIT-i method.
567 The seaward hydraulic gradient (parameter i) is the most important variable controlling the
568 seawater toe location, provides the major source of fresh groundwater discharge to sea, and
569 reflects the resultant effects of recharge rate, pumping rate, head of freshwater, freshwater
570 flux to the sea, sea level rise, and changing in transmissivity of aquifer. The GALDIT
571 method doesn't consider this parameter as input. On the Other hand, one of possible
572 challenge accompanied by serving the parameter i for parameter L in the GAiDIT method
573 may occur in delineating vulnerability of inland zones with a low spatial variation of
574 groundwater level (even inland groundwater level) driven by the low impact of
575 recharge/discharge components. In such regions, the small values of the hydraulic gradient
576 (i) may lead to inaccurate estimation of the final vulnerability index. Thus, the results of
577 GAiDIT method are more reliable for estimation of vulnerable zones due to time-
578 dependent anthropogenic changes (e.g., pumping). Results of this study indicated that
579 utilization of both parameters L and i in GALDIT-i approach may produce more accurate
580 vulnerability map which is more correlated to the four groundwater indices of f_{sea}, GQI,
581 TDS, and L_x. However, increasing the number of input parameters, compared with the
582 GAiDIT and GALDIT, may be one of drawback accompanied by the GALDIT-i index.
583 The results of the study can serve as a primary target for the introduction of future
584 mitigation and adaptation strategies on the indicators involving for vulnerability mapping
585 of coastal aquifers to SWI towards sustainable groundwater management. The detailed
586 vulnerability assessment could be built upon by carrying out numerical modeling in
587 aquifers identified accurately as being highly vulnerable by the index method.
588

5. Acknowledgements

The authors wish to thank the Editor-in-Chief, Professor Geoff Syme and two anonymous reviewers for their valuable comments which helped to improve the final manuscript. The authors Behzad Ataie-Ashtiani and Craig T. Simmons acknowledge support from the National Centre for Groundwater Research and Training, Australia. Behzad Ataie-Ashtiani appreciates the support of the Research office of the Sharif University of Technology, Iran. The authors also appreciate the Guilan Regional Water Authority for providing the required data of this paper.

6. Nomenclatures

SWI	SWI seawater intrusion
SLR	Sea level rise
MSL	Mean sea level
PCC	Pearson's correlation coefficient
As-Ko	Astaneh-Koochesfahan aquifer
La-Ch	Lahijan-Chaboksar
$\overline{\mathrm{GQI}}$ [ML^{-3}]	Average of $\mathrm{GQI}_{\mathrm{mix}}$ and $\mathrm{GQI}_{\mathrm{dom}}$
TC [ML^{-3}]	Concentration of total cations in groundwater
TA [ML^{-3}]	Concentration of total anions in groundwater
E	Electrical Conductivity of seawater
TDS	Total dissolved solids
PV [$-$]	Percentage of variation in the vulnerability index
dh [$-$]	Difference of hydraulic head in coastal aquifer
dx [$-$]	Horizontal difference of two points in coastal aquifer
G [$-$]	Groundwater occurrence (aquifer type)
A [L^2]	Area of aquifer plain
L [L]	Height of groundwater level above sea level
D [L]	Distance from the shore line
I [$-$]	Impact of the existing status of seawater intrusion
T [$-$]	Aquifer saturated thickness
i [$-$]	Hydraulic gradient of freshwater in coastal aquifer
x [L]	Distance taken from the coastline

$K\ [L\ T^{-1}]$	Saturated hydraulic conductivity of aquifer formations
$B\ [L]$	Saturated thickness of aquifer
$T\ [L^2T^{-1}]$	Transmissivity of aquifer
$\bar{P}\ [L]$	Average annual rainfall on the aquifer plain
$\mathrm{GQI_{mix}}\ [-]$	Mixed groundwater quality index
$\mathrm{GQI_{dom}}\ [-]$	Domestic groundwater quality index
$\mathrm{Vul_j}\ [-]$	Vulnerability score affected by changes in specific indicator j
$\mathrm{Vul_0}\ [-]$	Vulnerability score for the initial condition
$\mathrm{Cl_i}\ [\mathrm{ML^{-3}}]$	Concentration of chloride ion in groundwater
$\mathrm{Cl_{fw}}\ [\mathrm{ML^{-3}}]$	Concentration of chloride ion in freshwater
$\mathrm{Cl_{sw}}\ [\mathrm{ML^{-3}}]$	Concentration of chloride ion in seawater
$\mathrm{HCO_3^-}\ [\mathrm{ML^{-3}}]$	Concentration of bicarbonate ion in groundwater
$\mathrm{CO_3^{2-}}\ [\mathrm{ML^{-3}}]$	Concentration of carbonate ion in groundwater
$\mathrm{Na^+}\ [\mathrm{ML^{-3}}]$	Concentration of sodium ion in groundwater
$\mathrm{Ca^{2+}}\ [\mathrm{ML^{-3}}]$	Concentration of calcium ion in groundwater
$\mathrm{Mg^{2+}}\ [\mathrm{ML^{-3}}]$	Concentration of Magnesium ion in groundwater
$\mathrm{SO_4^{2-}}\ [\mathrm{ML^{-3}}]$	Concentration of sulfate ion in groundwater
$R_i\ [-]$	Rating value for each for different hydrogeological parameter setting
$W_i\ [-]$	Weight of different hydrogeological parameter setting
$\mathrm{h_{SW}}\ [L]$	Seaward hydraulic head
$\mathrm{h_{LW}}\ [L]$	Landward hydraulic head
$L_x\ [L]$	Length of the seawater intrusion at point x from shoreline
$q'\ [L^2T^{-1}]$	Freshwater groundwater discharge to the sea
$h_{f_x}\ [L]$	Freshwater hydraulic head above the MSL in each distance x from shore-line
$h_x\ [L]$	Thickness of freshwater above the interface in each distance x from shoreline
$h_0\ [L]$	Saturated aquifer thickness
$W_{net}\ [L\ T^{-1}]$	Net recharge to aquifer
$z_0\ [L]$	Depth to horizontal base of the aquifer below the MSL
$L_T\ [L]$	Seawater toe location from shoreline
$q_b\ [L^2T^{-1}]$	Regional flux entered from landward boundary
$\mathrm{N_{piez}}\ [-]$	Number of piezometers to monitor the groundwater level
$\Delta h\ [L]$	Average annual variation of groundwater level

$\Delta V\ [L^3]$	Average annual variation of groundwater storage
$S_c\ [-]$	Storage coefficient of aquifer
$\mathrm{GW}_D\ [L]$	Depth to groundwater
$\mathrm{GW}_L\ [L]$	Groundwater level above MSL
$f_{sea}\ [-]$	Fraction of seawater in coastal aquifer
$\delta\ [-]$	Density difference ratio of the seawater and freshwater
$\rho_s\ [M\ L^{-3}]$	Sea-water density
$\rho_f\ [M\ L^{-3}]$	Freshwater density

7. References

Allen, L., Bennett, T., Lehr, J.H., Petty, R.J., and Hackett, G., 1987. DRASTIC: a standardized system for evaluating groundwater pollution potential using hydrogeologic settings. US EPA Report 600/2-87/035, Robert S. Kerr Environmental Research Laboratory, Ada, OK.

Allouche, N., Maanan, M., Gontara, M., Rollo, N., Jmal, I., and Bouri, S., 2017. A global risk approach to assessing groundwater vulnerability. Environmental Modelling & Software 88, 168-182. http://dx.doi.org/10.1016/j.envsoft.2016.11.023

Alongi, D.M., 1999. Coastal ecosystem processes. CRC Press, Florida.

Appelo C.A.J., and Willemsen, A., 1987. Geochemical calculations and observations on salt water intrusions, I. A combined geochemical/mixing cell model. J Hydrol. 94, 313–330. https://doi.org/10.1016/0022-1694(87)90058-8

Appelo, C.A., and Postma, D., 2005. Geochemistry, groundwater and pollution. Balkema, Leiden, The Netherlands.

Asadi, P., Hosseini, S.M., Ataie-Ashtiani, B., and Simmons, S.T., 2017. Fuzzy vulnerability mapping of urban groundwater systems to nitrate contamination. Environmental Modeling & Software 96(1), 146-157. https://doi.org/10.1016/j.envsoft.2017.06.043

Ataie-Ashtiani, B., Rajabi, M.M., Ketabchi, H., 2013a. Inverse modeling for freshwater lens in small islands: Kish Island, Persian Gulf. Hydrol. Process. 27, 2759–2773. https://doi.org/10.1002/hyp.9411

Ataie-Ashtiani, B., Volker, R.E., Lockington, D.A., 1999. Tidal effects on seawater intrusion in unconfined aquifers. J. Hydrol. 216 (1–2), 17–31. https://doi.org/10.1016/S0022-1694(98)00275-3

Ataie-Ashtiani, B., Volker, R.E., Lockington, D.A., 2001. Tidal effects on groundwater dynamics in unconfined aquifers. Hydrol. Process. 15 (4), 655–669. https://doi.org/10.1002/hyp.183

Ataie-Ashtiani, B., Werner, A.D., Simmons, C.T., Morgan, L.K., Lu, C., 2013b. How important is the impact of land-surface inundation on seawater intrusion caused by sea-level rise? Hydrogeol. J. 21 (7), 1673–1677. https://doi.org/10.1007/s10040-013-1021-0

Badaruddin, S., Werner, A.D., Morgan, L.K., 2015. Water table salinization due to seawater intrusion. Water Resour. Res. 51 (10), 8397–8408. https://doi.org/10.1002/2015WR017098

Baena-Ruiz, L., Pulido-Velazquez, D., Collados-Lara, A. J., Renau-Pruñonosa, A., and Morell, I., 2018. Global assessment of seawater intrusion problems (status and vulnerability). Water Resources Management, 32(8), 2681-2700. https://doi.org/10.1007/s11269-018-1952-2

630 Beljin, M., R. Ross, AND S. Acree. 3PE: A Tool for Estimating Groundwater Flow Vectors. U.S.
631 Environmental Protection Agency, Washington, DC, EPA/600/R-14/273, 2014.
632 Belsley, D.A., Kuh, E., and Welsch, R.E. 1980. Regression Diagnostics: Identifying Influential Data and
633 Sources of Collinearity. New York: John Wiley and Sons.
634 Bouderbala, A., Remini, B., Hamoudi, A.S., and Pulido-Bosch, A., 2016. Assessment of groundwater
635 vulnerability and quality in coastal aquifers: a case study (Tipaza, North Algeria). Arab J Geosci. 9, 181.
636 https://doi.org/10.1007/s12517-015-2151-6
637 Chachadi, A.G., 2005. Seawater intrusion mapping using modified GALDIT indicator model—case study in
638 Goa. Jalvigyan Sameeksha 20, 29–45.
639 Chachadi, A.G., Lobo-Ferreira, J.P., 2001. Sea water intrusion vulnerability mapping of aquifers using
640 GALDIT method. Coastin—A Coast. Policy Res. Newsl. 4, 7–9.
641 Chachadi, A.G., Lobo-Ferreira, J.P., 2007. Assessing aquifer vulnerability to seawater intrusion using
642 GALDIT method: part 2, GALDIT indicators description. Water Celt Countries Quant QualClim Var.
643 310, pp. 172–180.
644 Comte, J.C., Cassidy, R., Obando, J., Robins, N., Ibrahim, K., Melchioly, S., Mjemah, I., Shauri, H.,
645 Bourhane, A., Mohamed, I. and Noe, C., 2016. Challenges in groundwater resource management in
646 coastal aquifers of East Africa: Investigations and lessons learnt in the Comoros Islands, Kenya and
647 Tanzania. Journal of Hydrology: Regional Studies, 5, pp.179-199.
648 https://doi.org/10.1016/j.ejrh.2015.12.065
649 Cook, P.G., Dogramaci, S., McCallum, J.L. and Hedley, J., 2017. Groundwater age, mixing and flow rates in
650 the vicinity of large open pit mines, Pilbara region, northwestern Australia. Hydrogeology Journal 25(1),
651 39–53.
652 Costanza, R., d'Arge, R., de Groot, R., Farber, S., Grasso, M., Hannon, B., Limburg, K., Naeem, S., O'Neill,
653 R.V., Paruelo, J., Raskin, R.G., Sutton, P., and van den Belt M., 1997. The value of the world's
654 ecosystem services and natural capital. Nature 387, 253–260.
655 Crossland, Ch.J., Baird, Dan, Ducrotoy, J.P.A., Lindeboom, H.J., Buddemeier, R.W., Dennison, W.C.,
656 Maxwell, B.A., Smith, S.V., Swaney, D.P. 2003. The Coastal Zone – a Domain of Global Interactions. In
657 Coastal Fluxes in the Anthropocene: The Land-Ocean Interactions in the Coastal Zone Project of the
658 International Geosphere-Biosphere Programme (pp.1-37).
659 Davis, C.J., 1987. Planning timber harvest activities with geographic information/decision support systems.
660 PhD Thesis, Department of Forestry and Natural Resources, Purdue University, West Lafayette, IN., pp:
661 249.
662 Docheshmeh-Gorji, A., Asghari-Moghaddam, A., 2016. Vulnerability assessment of saltwater intrusion using
663 simplified GAPDIT method: a case study of Azarshahr Plain Aquifer. East. Arab. J. Geosci. 9, 1–13.
664 https://doi.org/10.1007/s12517-015-2200-1
665 Dörfliger, N., Dumon, A., Aunay, B., Picot, G., Moynot, C., and Bollard, M., 2011. Influence de la montée
666 du niveau de la mer sur le biseau salin des aquifères côtiers des DROM/COM, Rapport final [Influence of
667 rising sea levels on the salt wedge of coastal aquifers of the DROM/COM, Final report]. BRGM RP-
668 60828-FR. BRGM, Orléans, France. http://www.onema.fr/IMG/pdf/2011_047-2.pdf. Accessed 12 June
669 2015.

Ferguson, G., and Gleeson, T., 2012. Vulnerability of coastal aquifers to groundwater use and climate change. Nature Climate Change, 2(5), 342.

Fernandino, G., Elliff, C.I., and Silva, I.R., 2018. Ecosystem-based management of coastal zones in face of climate change impacts: Challenges and inequalities. Journal of Environmental Management 215, 32-39. https://doi.org/10.1016/j.jenvman.2018.03.034

Fetter Jr., C.W., 1973. Water resources management in coastal plain aquifers. In: Chow, V.T. (Ed.), Water for the Human Environment: Proceedings of the First World Congress on Water Resources. International Water Resources Association, Illinois, pp. 322–331.

Fetter, C.W., 2001. Applied Hydrogeology, fourth ed. Prentice Hall Inc., New Jersey, 598p.

Fuentesa, J.C.N., Granados, P.A., and Martins F.C., 2018. Integrated coastal management in Campeche, Mexico; a review after the Mexican marine and coastal national policy. Ocean and Coastal Management 154, 34–45. https://doi.org/10.1016/j.ocecoaman.2017.12.029

Geological Survey & Mineral Explorations of Iran (GSI). 1997. Geology map of the Mazandaran Province.

Gholami, V., Yousefi, Z., and Rostami, H.Z., 2010. Modeling of ground water salinity on the Caspian southern coasts. Water Resour. Manag. 24, 1415–1424.

Ghyben, W.B., 1888. Notes on the probable resultsof well drilling near Amsterdam. Tijdschr. van het K. Inst. van Ingenieur. Hague 9, 8–22.

Ghyben, W.B., 1889. Nota in Verband met de Voorgenomen Putboring Nabij Amsterdam [Memorandum related to planned well drilling near Amsterdam]. Tijdschr Koninhitk Inst Ing 9, 8-22.

Golshan, M., Colombani, N., and Mastrocicco, M., 2018. Assessing Aquifer Salinization with Multiple Techniques along the Southern Caspian Sea Shore (Iran). Water 10(348), 2-17. https://doi.org/10.3390/w10040348

Gonneea, M.E., Mulligan, A.E., and Charette, M.A., 2013. Climate-driven sea level anomalies modulate coastal groundwater dynamics and discharge. Geophysical Research Letters, 40(11), 2701-2706. https://doi.org/10.1002/grl.50192,2013

Guilan Regional Water Authority, GRWA, Qualitative and quantitative studying of plains with groundwater monitoring networks: Fomanat, Lahijan-Chaboksar, and Astaneh-Koochesfahan plains. Report No. 8353/111, release: Jan 2015, 340 pp.

Herzberg, A., 1901. Die Wasserversorgung einiger Nordseebader [the water supply of the North Sea coast in Germany]. Z Gasbeleucht Wasserversorg 44, 815–819.

Holding, S., and Allen, D.M., 2015. From days to decades: numerical modeling of freshwater lens response to climate change stressors on small islands. Hydrol. Earth Syst. Sci. 19, 933–949. https://doi.org/10.5194/hess-19-933-2015

Jahanshahi, R., Zare, M., 2016. Hydrochemical investigations for delineating saltwater intrusion into the coastal aquifer of Maharlou Lake. Iran J. African Earth Sci. 121, 16–29. https://doi.org/10.1016/j.jafrearsci.2016.05.014

Kallioras, A., Pliakas, F., Skias, S., Gkiougkis, I., 2011. Groundwater vulnerability assessment at SW Rhodope aquifer system in NE Greece. In: Lambrakis N, Stournaras G, Katsanou (eds) Advances in the research of aquatic environment. Environ Earth Sci. Springer 2:351–358. https://doi.org/10.1007/978-3-642-24076-8_41

Kantamaneni, K., 2016. Coastal infrastructure vulnerability: an integrated assessment model. Nat. Hazards 84, 139–154.

Kazakis, N., Spiliotis, M., Voudouris, K., Pliakas, F.K., and Papadopoulos, B., 2018. A fuzzy multicriteria categorization of the GALDIT method to assess seawater intrusion vulnerability of coastal aquifers. Science of the kironment 621, 524–534. https://doi.org/10.1016/j.scitotenv.2017.11.235

Ketabchi, H., Ataie-Ashtiani, B., 2015. Review: coastal groundwater optimization—advances, challenges, and practical solutions. Hydrogeol. J. 23 (6), 1129–1154. https://doi.org/10.1007/s10040-015-1254-1

Ketabchi, H., Mahmoodzadeh, D., Ataie-Ashtiani, B., and Simmons, C.T., 2010. Sea-level rise impacts on seawater intrusion in coastal aquifers: Review and integration. Journal of Hydrology 535, 235–255. https://doi.org/10.1016/j.jhydrol.2016.01.083

Ketabchi, H., Mahmoodzadeh, D., Ataie-Ashtiani, B., Werner, A.D., Simmons, C.T., 2014. Sea-level rise impact on fresh groundwater lenses in two-layer small islands. Hydrol. Process. 28, 5938–5953. https://doi.org/10.1002/hyp.10059

Klassen, J., Allen, D.M., 2017. Assessing the Risk of Saltwater Intrusion in Coastal Aquifers. J. Hydrol. 551, 730-745. https://doi.org/10.1016/j.jhydrol.2017.02.044

Klassen, J., and Allen, D.M., 2017. Assessing the risk of saltwater intrusion in coastal aquifers. Journal of Hydrology 551,730–745. https://doi.org/10.1016/j.jhydrol.2017.02.044

Kosarev, A.N., and Yablonskaya, E.A., 1994. The Caspian Sea; SPB Academic Publishing: The Hague, The Netherlands, p. 259. ISBN 9051030886.

Kura, N.U., Ramli, M.F., Ibrahim, S., Sulaiman, W.N.A., Aris, A.Z., Tanko, A.I., Zaudi, M. A., 2014b. Assessment of groundwater vulnerability to anthropogenic pollution and seawater intrusion in a small tropical island using index-based methods. Environ. Sci. Pollut. Res. 22, 1512–1533. https://doi.org/10.1007/s11356-014-3444-0

Kura, N.U., Ramli, M.F.., Ibrahim, Sh., Sulaiman, W.N.A., Aris, A.Z., Tanko, A.I., and Zaudi, M.A., 2014. Assessment of groundwater vulnerability to anthropogenic pollution and seawater intrusion in a small tropical island using index-based methods. Environ Sci Pollut Res. https://doi.org/10.1007/s11356-014-3444-0

Leroy, S.A.G., Marret, F., Gibert, E., Chalié, F., Reyss, J.L., and Arpe, K., 2007. River inflow and salinity changes in the Caspian Sea during the last 5500 years. Quat. Sci. Rev. 26, 3359–3383.

Li, R., and Merchant, J.W., 2013. Modeling vulnerability of groundwater to pollution under future scenarios of climate change and biofuels-related land use change: a case study in north Dakota, USA. Sci Total Environ. 447, 32-45. https://doi.org/10.1016/j.scitotenv.2013.01.011

Loaciga, H.A., Pingel, T.J., and Garcia, E.S., 2012. Sea water intrusion by sea-level rise: scenarios for the 21st century. Groundwater 50, 37-47. https://doi.org/10.1111/j.1745-6584.2011.00800.x

Lobo-Ferreira, J.P., Chachadi, A.G., Diamantino, C., and Henriques, M.J., 2005. Assessing aquifer vulnerability to seawater intrusion using GALDIT method: part 1—application to the Portuguese aquifer of Monte Gordo, The fourth inter-Celtic colloquium on hydrology and management of water resources, Guimaraes, Portugal, 12 p.

Lobo-Ferreira, J.P., Chachadi, A.G., Diamantino, C., Henriques, M.J., 2007. Assessing aquifer vulnerability to seawater intrusion using the GALDIT method: Part 1 – application to the Portuguese Monte Gordo

aquifer. In: Lobo Ferreira, J.P., Viera, J.M.P. (Eds.), Proceedings of Water in Celtic Countries: Quantity, Quality and Climate Variability, IAHS Publication 310. International Association of Hydrological Sciences, Wallingford, pp. 161–171.

Luoma, S., Okkonen, J., and Korkka-Niemi, K., 2017. Comparison of the AVI, modified SINTACS and GALDIT vulnerability methods under future climate-change scenarios for a shallow low-lying coastal aquifer in southern Finland. Hydrogeol J. 25, 203–222. https://doi.org/10.1007/s10040-016-1471-2

Mahesha, A., Vyshali, A.M., Lathashri, U.A., and Ramesh, H., 2012. Parameter Estimation and Vulnerability Assessment of Coastal Unconfined Aquifer to Saltwater Intrusion. Journal of Hydrologic Engineering 17(8), 933-943. https://doi.org/10.1061/(ASCE)HE.1943-5584.0000524

Mahmoodzadeh, D., Ketabchi, H., Ataie-Ashtiani, B., Simmons, C.T., 2014. Conceptualization of a fresh groundwater lens influenced by climate change: a modeling study of an arid-region island in the Persian Gulf, Iran. J. Hydrol. 519, 399–413. https://doi.org/10.1016/j.jhydrol.2014.07.010

McMillan, L.A., Rivett, M.O., Tellam, J.H., Dumble, P., and Sharp, H. 2014. Influence of vertical flows in wells on groundwater sampling. Journal of Contaminant Hydrology 169, 50–61.

Morgan, L.K., Bakker, M., Werner, A.D., 2015. Occurrence of seawater intrusion overshoot. Water Resour. Res. 51 (4), 1989–1999. https://doi.org/10.1002/2014WR016329

Morgan, L.K., Werner, A.D., Simmons, C.T., 2012. On the interpretation of coastal aquifer water level trends and water balances: a precautionary note. J. Hydrol. 470–471, 280–288. https://doi.org/10.1016/j.jhydrol.2012.09.001

Motevalli, A.R., Moradi H.R., and Javadi, S., 2018. A Comprehensive evaluation of groundwater vulnerability to saltwater up-coning and sea water intrusion in a coastal aquifer (case study: Ghaemshahr-juybar aquifer). Journal of Hydrology 557, 753–773. https://doi.org/10.1016/j.jhydrol.2017.12.047

Najib, S., Fadili, A., Mehdi, K., Riss, J., Makan, A., Guessir, H., 2016. Salinization process and coastal groundwater quality in Chaouia Morocco. J. Afr. Earth Sci. 115, 17–31. https://doi.org/10.1016/j.jafrearsci.2015.12.010

Nofal, E.R., Amerb, M.A., El-Didy, S.M., and Fekry, A.M., 2015. Delineation and modeling of seawater intrusion into the Nile DeltaAquifer: A new perspective. Water Science 29, 156–166. https://doi.org/10.1016/j.wsj.2015.11.003

Özyurt, G.,and Ergin, A., 2007. Improving Coastal Vulnerability Assessments to Sea-Level Rise: A New Indicator-Based Methodology for Decision Makers. Journal of Coastal Research 26(2), 265 – 273. https://doi.org/10.2112/08-1055.1

Panagopoulos, G.P., Antonakos, A.K., and Lambrakis, N.J., 2006. Optimization of the DRASTIC method for groundwater vulnerability assessment via the use of simple statistical methods and GIS. Hydrogeol. J. 14, 894–911. https://doi.org/10.1007/s10040-005-0008-x

Panteleit, B., Hamer, K., Kringel, R., Kessels, W., Schulz, H., 2011. Geochemical processes in the saltwaterefreshwater transition zone: comparing results of a sand tank experiment with field data. Environ. Earth Sci. 62(1), 77-91. https://doi.org/10.1007/s12665-010-0499-1

Parisi, A., Monno, V., and Fidelibus, M.D., 2018. Cascading vulnerability scenarios in the management of groundwater depletion and salinization in semi-arid areas. International Journal of Disaster Risk Reduction, In Press. https://doi.org/10.1016/j.ijdrr.2018.03.004

790 Pedreira, R., Kallioras, A. Pliakas, F., Gkiougkis, I., and Schuth, C., 2015. Groundwater vulnerability
791 assessment of a coastal aquifer system at River Nestos eastern Delta, Greece. Environ Earth Sci. 73,
792 6387–6415. https://doi.org/10.1007/s12665-014-3864-7
793 Piper, A.M., 1944. Trans. Am. Geophys. Union, 25, 914–923.
794 Poulsen, D.L., Cook, P.G., Simmons, C.T., McCallum, J.L., and Dogramaci, S., 2018. Effects of
795 intraborehole flow on purging and sampling long-screened or open wells. Groundwater.
796 https://doi.org/10.1111/gwat.12797
797 Recinos, N., Kallioras, A., Pliakas, F., and Schuth, C. , 2015. Application of GALDIT index to assess the
798 intrinsic vulnerability to seawater intrusion of coastal granular aquifers. Environ Earth Sci. 73:1017–
799 1032. https://doi.org/10.1007/s12665-014-3452-x
800 Revelle, R., 1941. Criteria for recognition of sea water in groundwater. Trans Am Geophys Union 22, 593–
801 597. https://doi.org/10.1029/TR022i003p00593
802 Richter, B.C., and Kreitler, C.W., 1993. Geochemical Techniques for Identifying Sources of Groundwater
803 Salinization, CRC Press, Boca Raton.
804 Rockware, Inc., 2010, RockWorks earth science and GIS software: accessed September 24, 2010, at
805 http://www.rockware.com/.
806 Saidi, S., Bouri, S., and Dhia, H.B., 2013. Groundwater management based on GIS techniques, chemical
807 indicators and vulnerability to seawater intrusion modelling: application to the Mahdia–Ksour Essaf
808 aquifer, Tunisia. Environ Earth Sci. 70(4), 1551-1568. https://doi.org/10.1007/s12665-013-2241-2
809 Sarath Prasanth, S., Magesh, N., Jitheshlal, K., Chandrasekar, N., Gangadhar, K., 2012. Evaluation of
810 groundwater quality and its suitability for drinking and agricultural use in the coastal stretch of alappuzha
811 district, kerala, india. Appl. Water Sci. 2 (3), 165-175. https://doi.org/10.1007/s13201-012-0042-5
812 Shi, H., and Singh, A., 2003. Status and interconnections of selected environmental issues in the global
813 coastal zones. Ambio 32(2),145–152.
814 Singhal, B., and Gupta, R.P., 2010. Applied Hydrogeology of Fractured Rocks. Springer.
815 Sophiya, M.S., and Syed, T.H., 2013. Assessment of vulnerability to seawater intrusion and potential
816 remediation measures for coastal aquifers: a case study from eastern India. Environ Earth Sci 70(3),
817 1197–1209. https://doi.org/10.1007/s12665-012-2206-x
818 SPSS Inc., 2001. SPSS 11.0 Advanced Models: Englewood Cliffs, NJ: Prentice Hall.
819 Strack, O.D.L., 1984. Three-dimensional streamlines in Dupuit–Forchheimer models. Water Resour. Res. 20,
820 812–822. https://doi.org/10.1029/WR020i007p00812
821 Strack, O.D.L., 1989. Groundwater Mechanics. Prentice Hall, Englewood Cliffs, NJ, USA.
822 Tan, W.J., Yang, Ch.F., Châteauc, P.A., Leed, M.T., and Chang, Y.Ch. 2018. Integrated coastal-zone
823 management for sustainable tourism using a decision support system based on system dynamics: A case
824 study of Cijin, Kaohsiung, Taiwan. Ocean & Coastal Management 153(1), 131-139.
825 https://doi.org/10.1016/j.ocecoaman.2017.12.012
826 Tomaszkiewicz, M., Abou Najm, M., El-Fadel, M., 2014. Development of a groundwater quality index for
827 seawater intrusion in coastal aquifers. Environ. Model. Softw. 57, 13–26.
828 https://doi.org/10.1016/j.envsoft.2014.03.010

Trabelsi, N., Triki, I., Hentati, I., and Zairi, M., 2016. Aquifer vulnerability and seawater intrusion risk using GALDIT, GQISWI and GIS: case of a coastal aquifer in Tunisia. Environ Earth Sci. 75:669. https://doi.org/10.1007/s12665-016-5459-y

UNESCO, 2003. The integrated strategic design plan for the coastal ocean observations module of the Global Ocean Observing System. GOOS Report No. 125, IOC Information Documents Series No. 1183.

Van Stempvoort, D., Ewert, L., and Wassenaar, L., 1992. AVI: A method for groundwater protection mapping in the prairie province of Canada. Prairie Province Water Board Report 114, Regina, SK.

Walther, M., Graf, T., Kolditz, O., Liedl, R., and Post, V., 2017. How significant is the slope of the sea-side boundary for modeling seawater intrusion in coastal aquifers? Journal of Hydrology 551, 648–659. https://doi.org/10.1016/j.jhydrol.2017.02.031

Werner, A.D., 2017. On the classification of seawater intrusion. Journal of Hydrology 551, 619–631. https://doi.org/10.1016/j.jhydrol.2016.12.012

Werner, A.D., Bakker, M., Post, V.E.A., Vandenbohede, A., Lu, C., Ataie-Ashtiani, B., Simmons, C.T., Barry, D.A., 2013. Seawater intrusion processes, investigation and management: recent advances and future challenges. Adv. Water Resour. 51, 3–26. https://doi.org/10.1016/j.advwatres.2012.03.004

Werner, A.D., Jakovovic, D., Simmons, C.T., 2009. Experimental observations of saltwater up-coning. J. Hydrol. 373, 230–241. https://doi.org/10.1016/j.jhydrol.2009.05.004

Werner, A.D., Ward, J.D., Morgan, L.K., Simmons, C.T., Robinson, N.I., and Teubner, M.D., 2012. Vulnerability Indicators of Sea Water Intrusion. Groundwater 50(1), 48-58. https://doi.org/ j.1745-6584.2011.00817.x

Werner, A.D.,Ward, J.D., Morgan, L.K., Simmons, C.T., Robinson, N.I., Teubner, M.D., 2012. Vulnerability indicators of sea water intrusion. Groundwater 50 (1), 48–58. https://doi.org/10.1111/j.1745-6584.2011.00817.x

Xiao, H., Wang, D., Hagen, S. C., Medeiros, S. C., and Hall, C. R., 2016. Assessing the impacts of sea-level rise and precipitation change on the surficial aquifer in the low-lying coastal alluvial plains and barrier islands, east-central Florida (USA), Hydrogeology Journal, 24(7), 1791-1806. https://doi.org/10.1007/s10040-016-1437-4

Yang, J., Graf, T., Herold, M., and Ptak, T., 2013. Modelling the effects of tides and storm surges on coastal aquifers using a coupled surface–subsurface approach. Journal of contaminant hydrology, 149, 61-75. https://doi.org/10.1016/j.jconhyd.2013.03.002

Zhou, X., 2011. A method for estimating the fresh wateresalt water interface with hydraulic heads in a coastal aquifer and its application. Geoscience Frontiers 2(2), 199-203. https://doi.org/10.1016/j.gsf.2011.02.003

Zonenshain, L.P., and Le Pichon, X., 1986. Deep basins on the Black Sea and Caspian Sea as remnants of Mesozoic back-arc basins. Tectonophysics, 123, 181-211. https://doi.org/10.1016/0040-1951(86)90197-6

Graphical Abstract

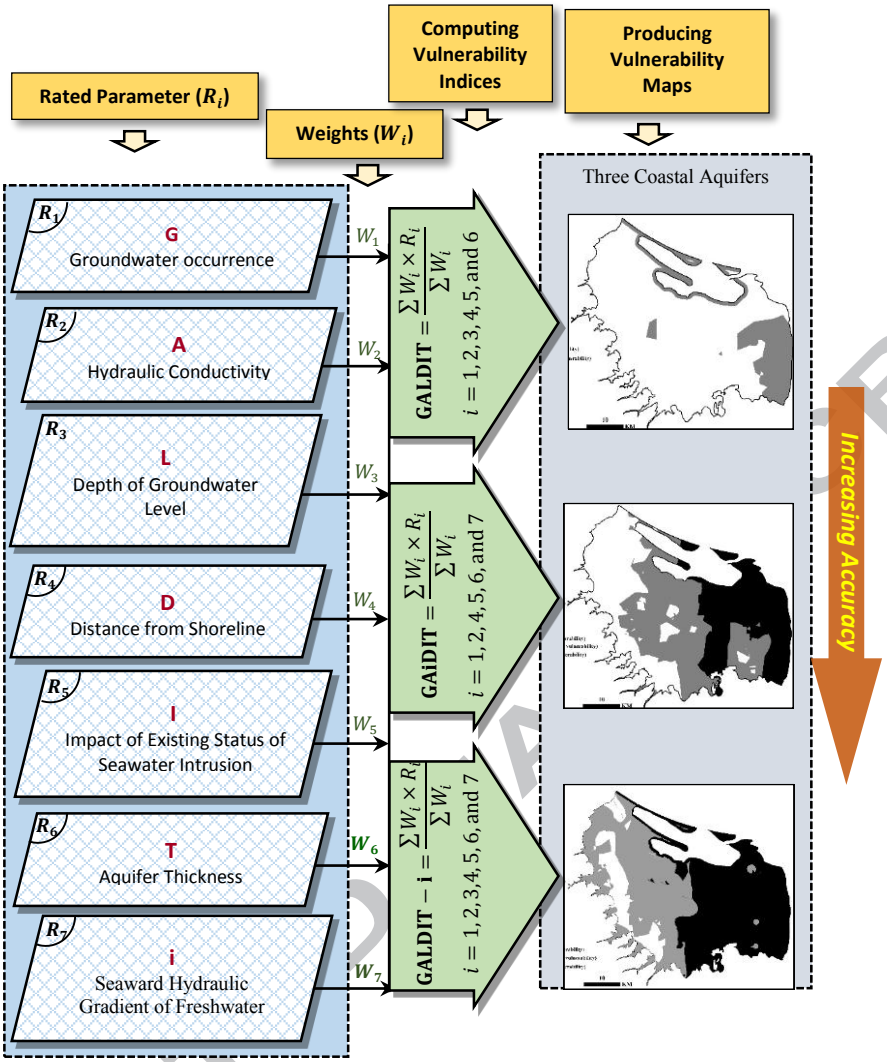

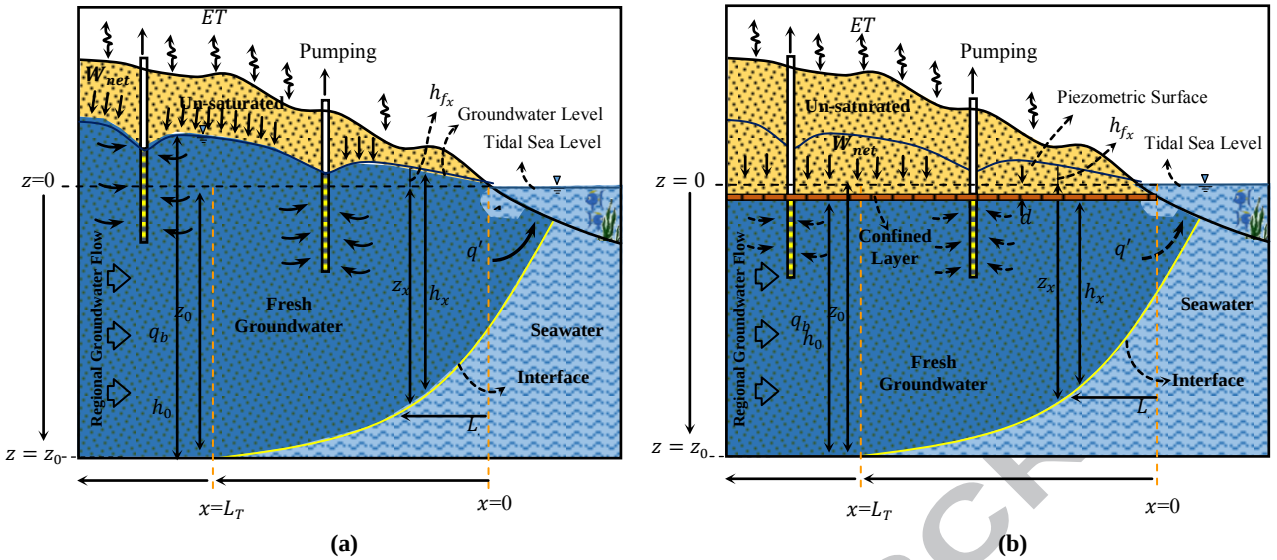

Fig. 1. Simplification of steady state sharp salt-fresh water interface for coastal aquifers: (a) unconfined aquifer, and (b) confined aquifer and definition of influenced parameters.

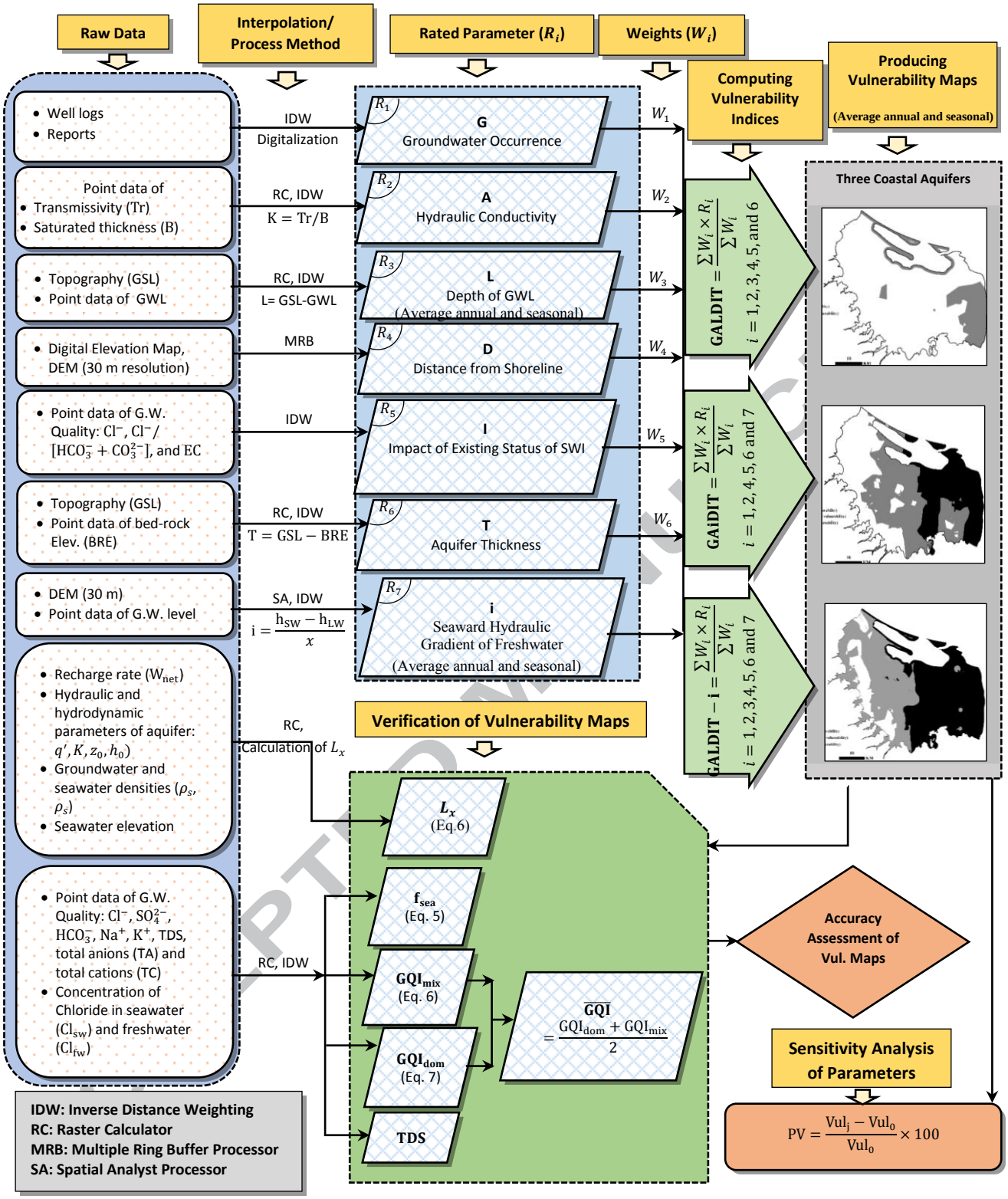

Fig. 2. Flow chart of methodology adopted in this study to assess three vulnerability indices, GALDIT, GAiDIT, and GALDIT-i.

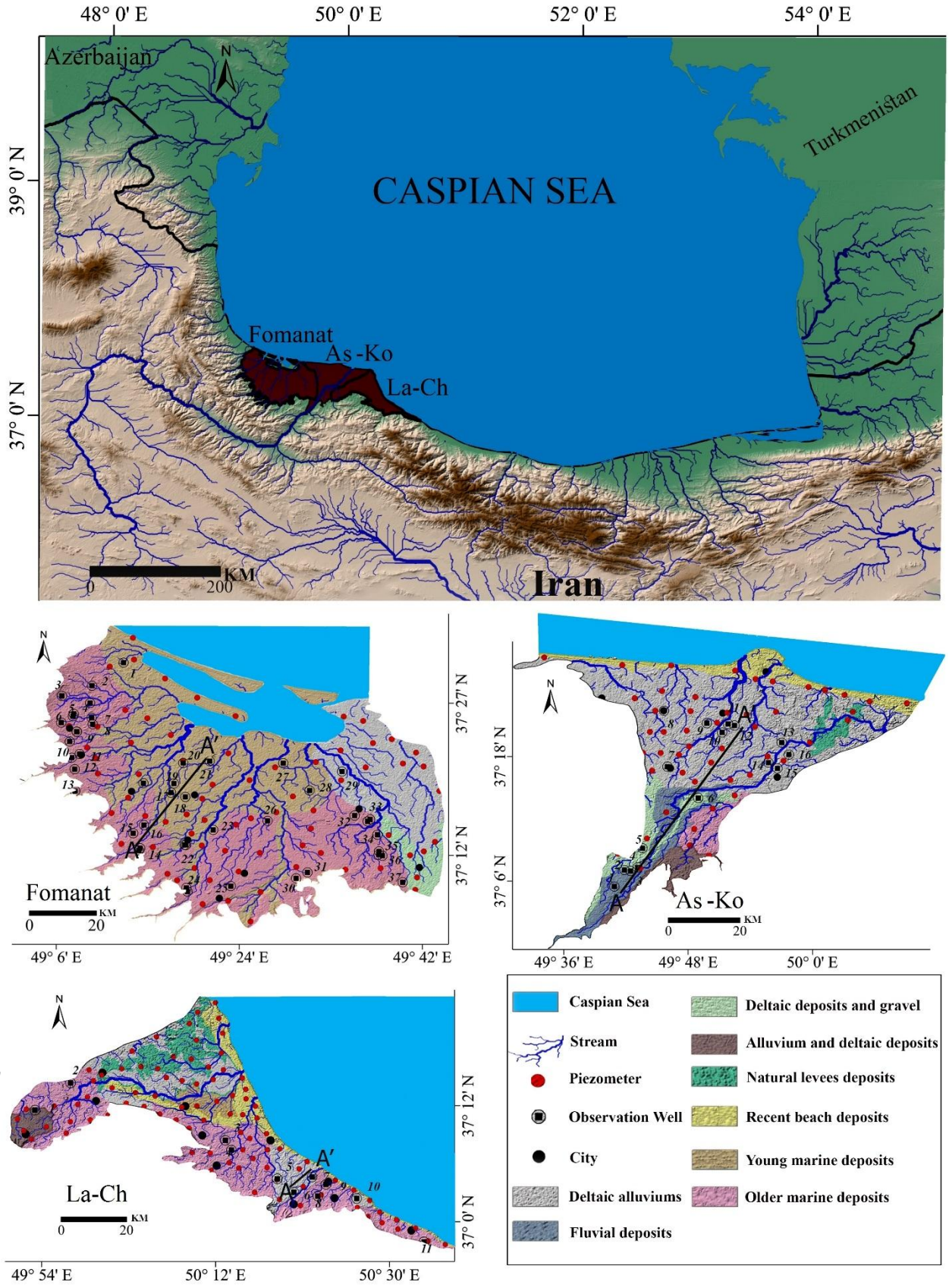

Fig. 3. Location of three studied aquifers: (A) Fomanat, (B) Astaneh-Koochesfahan (As-Ko), and (C) Lahijan-Chaboksar (La-Ch), exploration and piezometric wells. The geologic cross-section of aquifer along A-A′ is shown in Fig. 4.

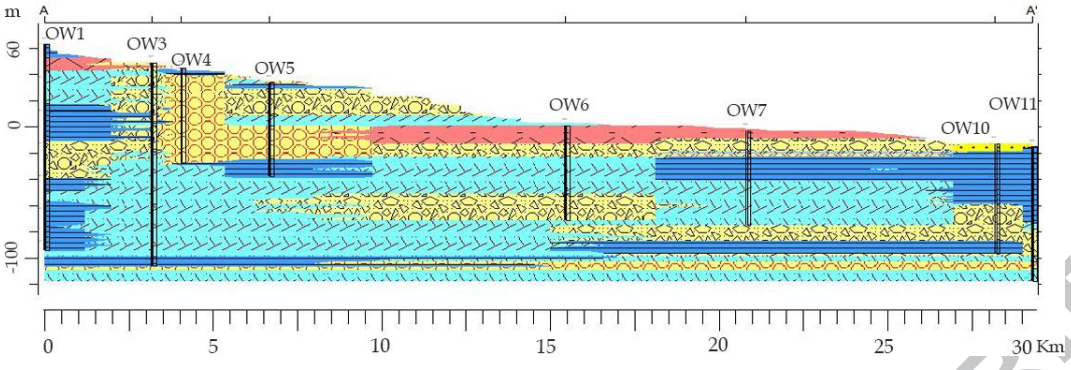

(a) Astaneh-Koochesfahan Aquifer (As-Ko)

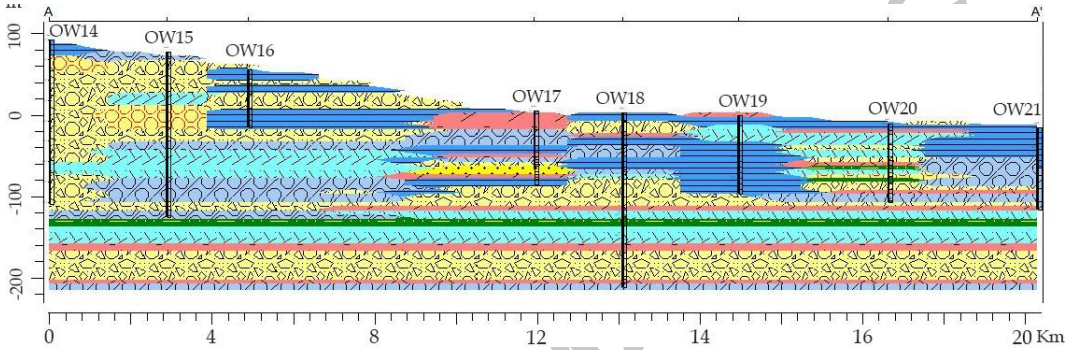

(b) Fomanat Aquifer

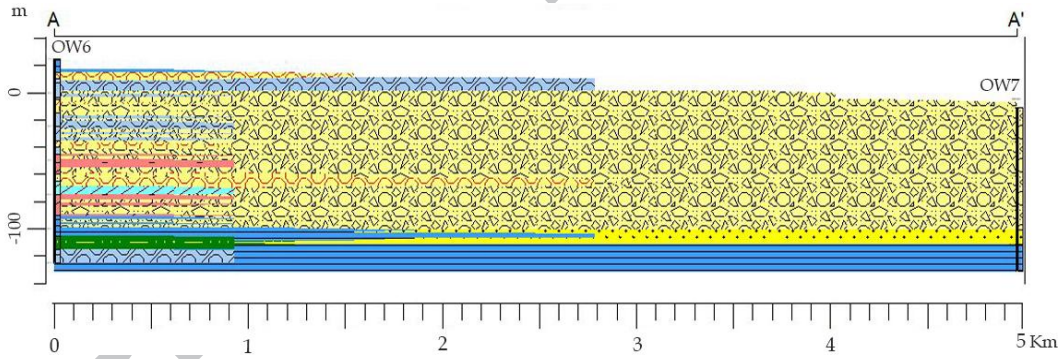

(c) Lahijan-Chaboksar Aquifer (La-Ch)

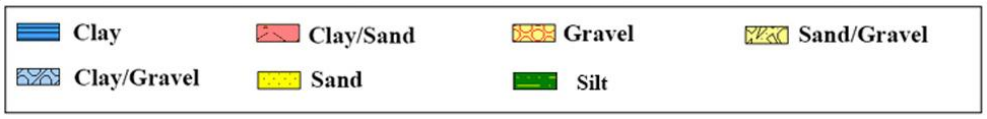

Fig. 4. Geologic cross-section of the studied aquifers along A-A' (see also Fig. 3). The figures are prepared by RockWorks software version 15 (www.rockware.com) by using the stratigraphy data of observation wells (OW) in each aquifer. The locations of observation wells in each cross-section are also shown in Fig. 3.

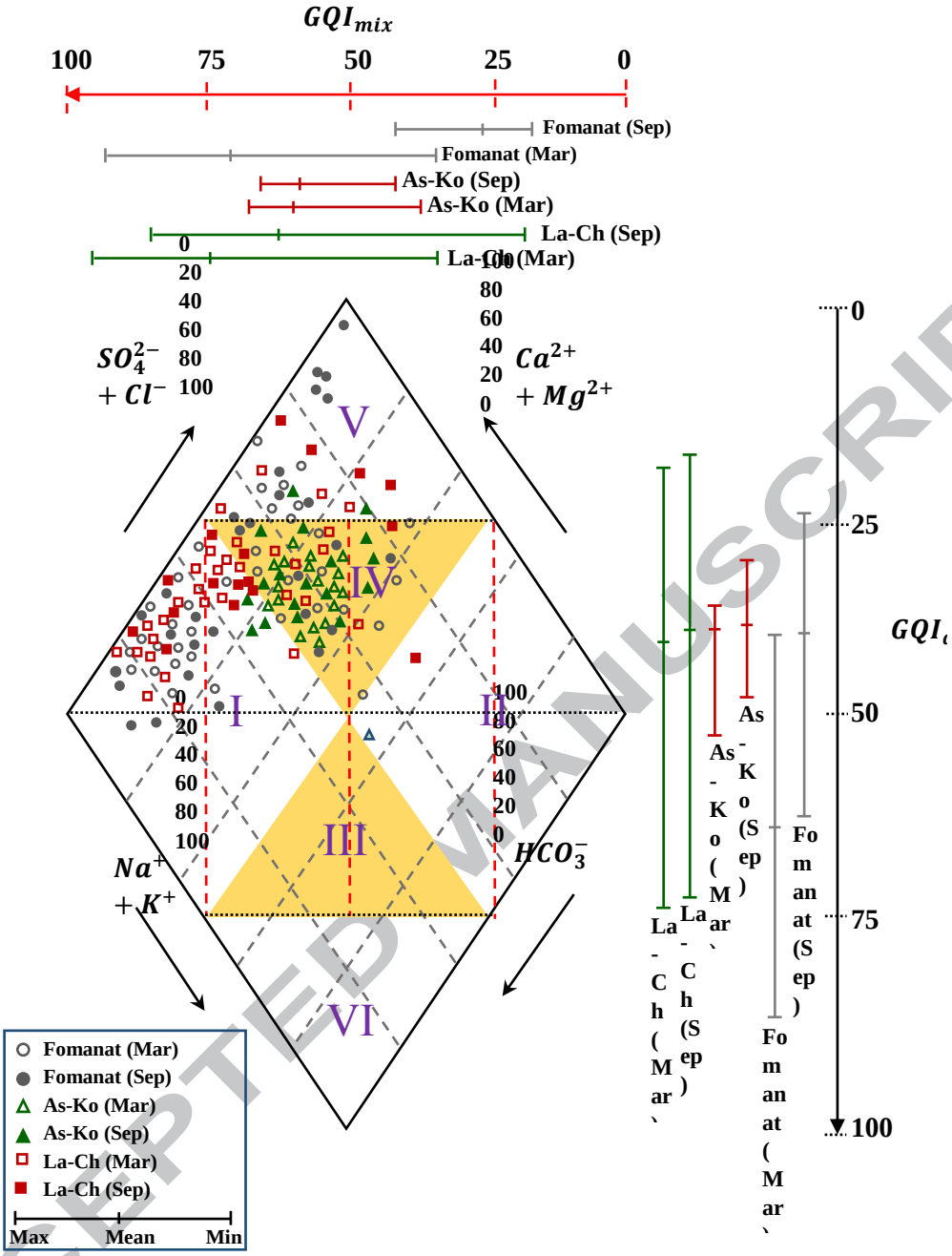

Fig. 5. Presentation of chemical quality data of groundwater data in three study aquifers on diamond field of Piper diagram, domains of groundwater classification, and calculated two groundwater quality indexes, GQI_{mix} and GQI_{dom} in two months of August and December.

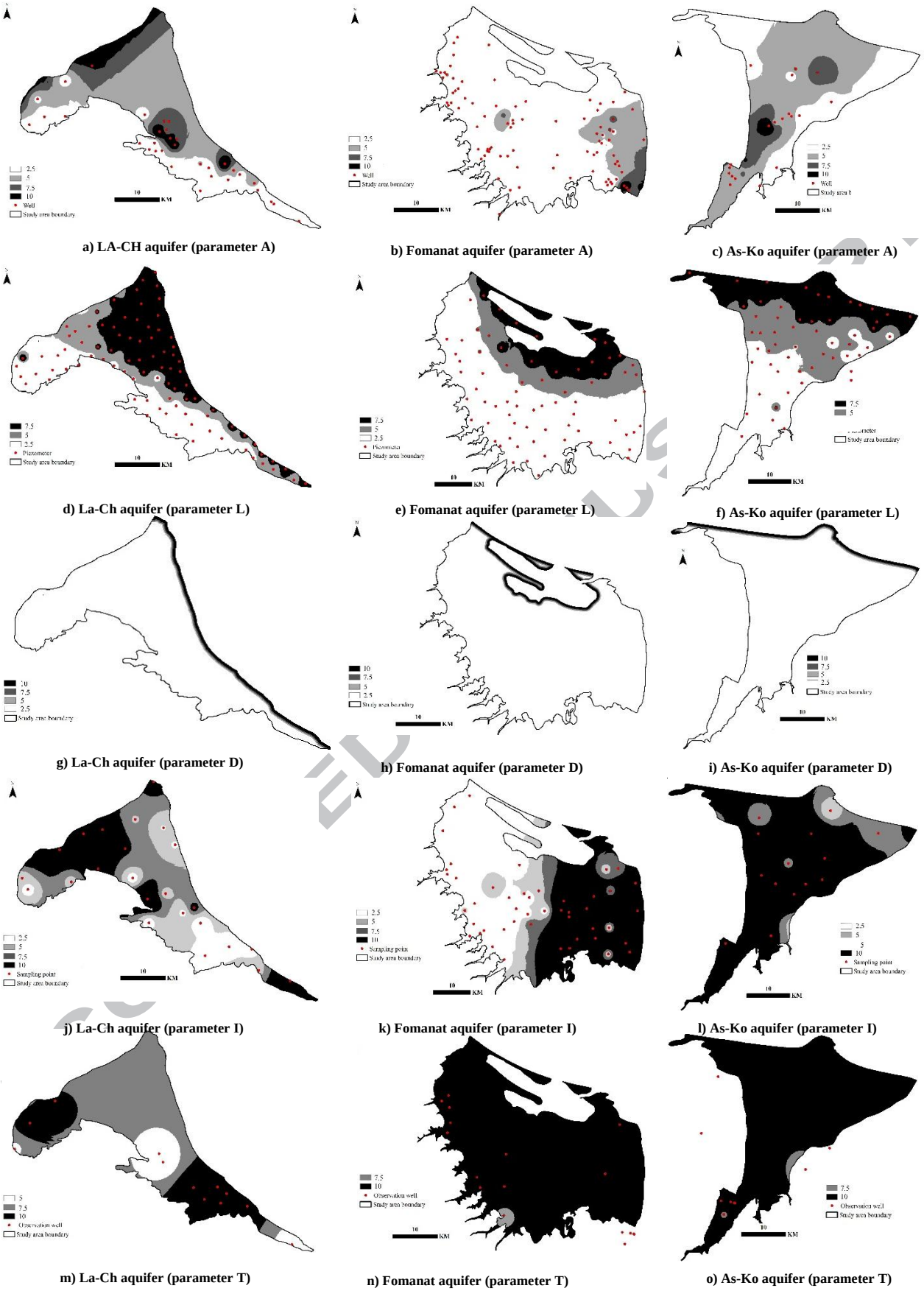

Fig. 6. Rated parameters of the GALDIT (parameters A, L, D, I, and T), GAiDIT (parameters A, i, D, I, and T), and GALDIT-i (parameters A, L, D, I, T, and i) methods. Figures of the parameter G (type of aquifer) are not shown, since the score of this parameter over three aquifers is 10. The parameter L and i have been rated based on annual average values of groundwater height above sea level and groundwater hydraulic gradient during 2013.

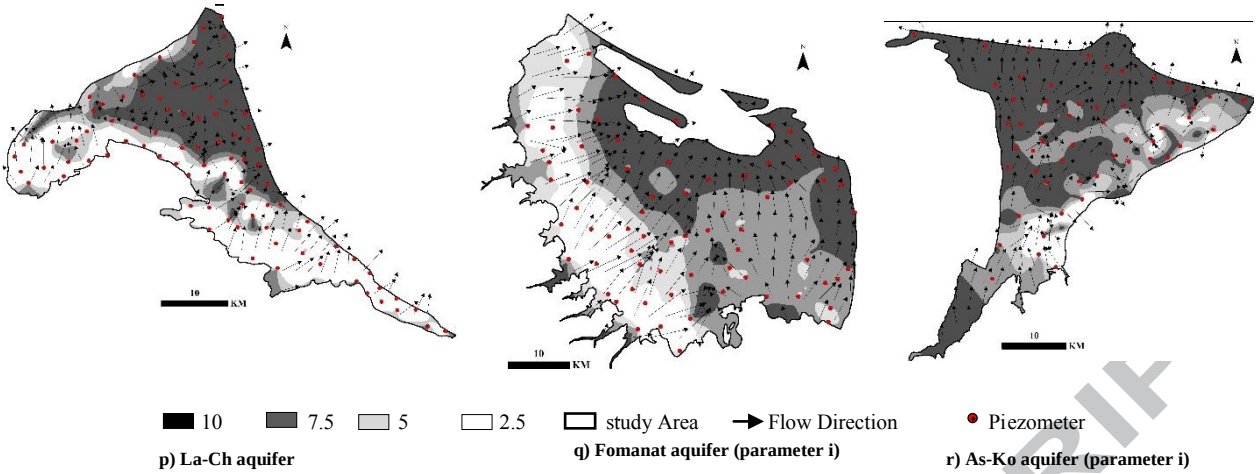

p) La-Ch aquifer **q) Fomanat aquifer (parameter i)** **r) As-Ko aquifer (parameter i)**

Fig. 6. *Continued*

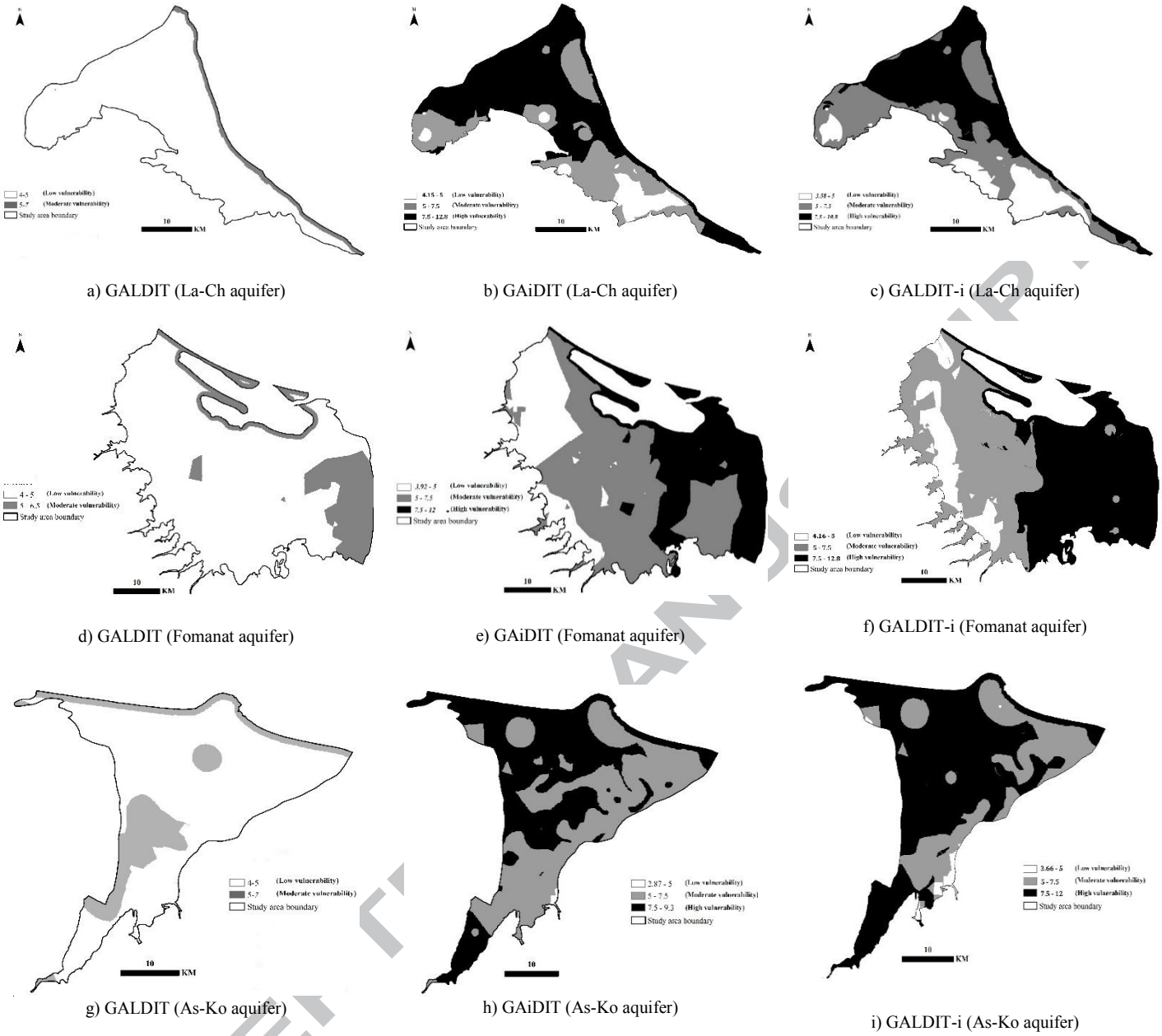

a) GALDIT (La-Ch aquifer) b) GAiDIT (La-Ch aquifer) c) GALDIT-i (La-Ch aquifer)

d) GALDIT (Fomanat aquifer) e) GAiDIT (Fomanat aquifer) f) GALDIT-i (Fomanat aquifer)

g) GALDIT (As-Ko aquifer) h) GAiDIT (As-Ko aquifer) i) GALDIT-i (As-Ko aquifer)

Fig. 7. Vulnerability maps of the three studied aquifers produced by GALDIT, GAiDIT, and GALDIT-i models based on annual-averaged data in 2013.

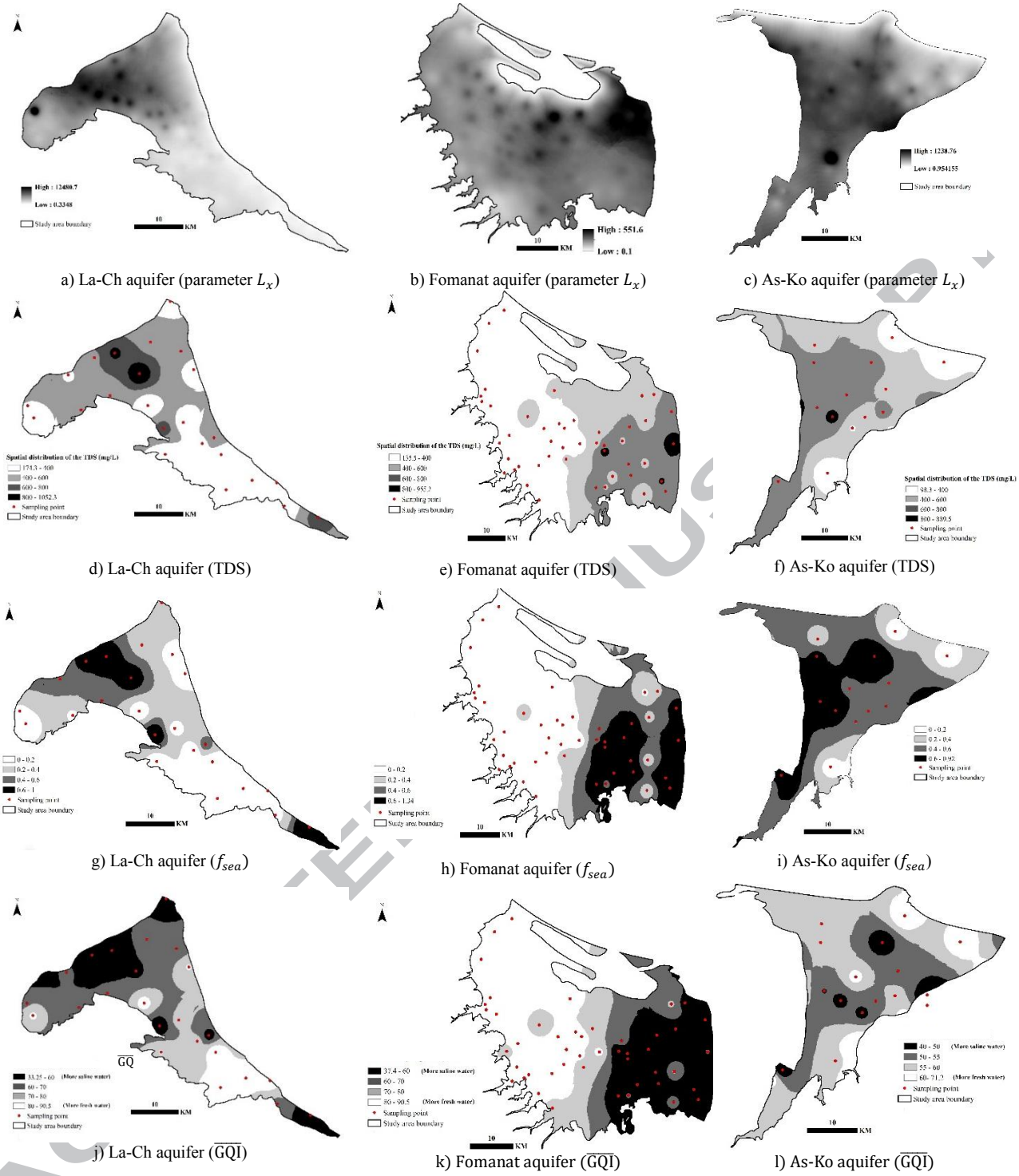

a) La-Ch aquifer (parameter L_x)
b) Fomanat aquifer (parameter L_x)
c) As-Ko aquifer (parameter L_x)
d) La-Ch aquifer (TDS)
e) Fomanat aquifer (TDS)
f) As-Ko aquifer (TDS)
g) La-Ch aquifer (f_{sea})
h) Fomanat aquifer (f_{sea})
i) As-Ko aquifer (f_{sea})
j) La-Ch aquifer ($\overline{\mathrm{GQI}}$)
k) Fomanat aquifer ($\overline{\mathrm{GQI}}$)
l) As-Ko aquifer ($\overline{\mathrm{GQI}}$)

Fig. 8. Distribution of L_x, TDS, f_{sea}, and the average value of $\mathrm{GQI_{mix}}$ and $\mathrm{GQI_{dom}}$ ($\overline{\mathrm{GQI}}$) over three studied aquifers.

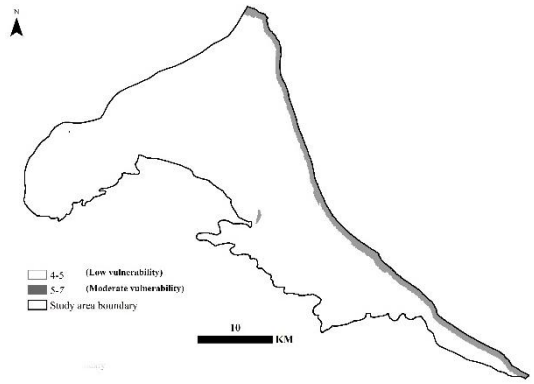

a) GALDIT (Dry Season)

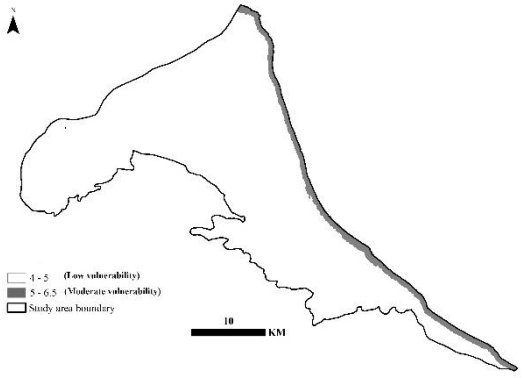

b) GALDIT (Wet Season)

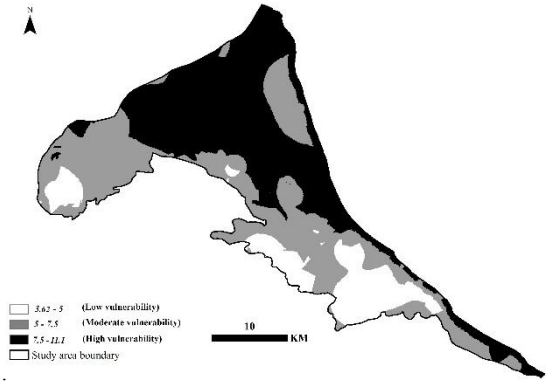

c) GAiDIT (Dry Season)

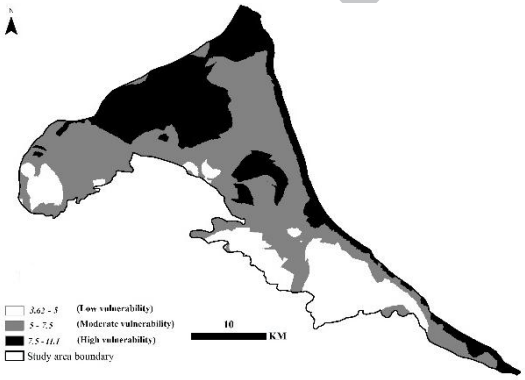

d) GAiDIT (Wet Season)

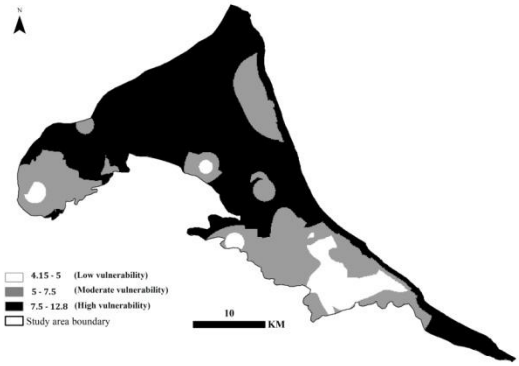

e) GALDIT-i (Dry Season)

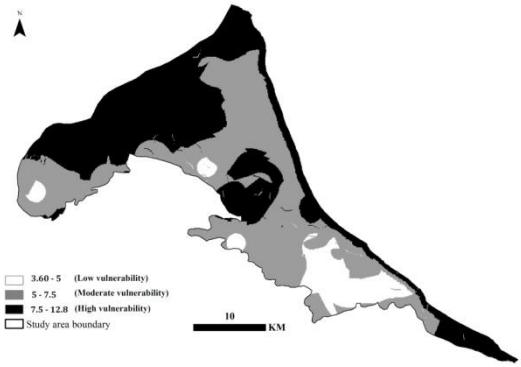

f) GALDIT-i (Wet Season)

Fig. 9. Vulnerability maps of La-Ch aquifer produced by GALDIT, GAiDIT, and GALDIT-i methods based on corresponding data of dry (September) and wet (March) seasons.

Table 1. Summary of recent studies relating to overlay/index methods (O/I) adopted for vulnerability mapping of coastal aquifers to SWI.

Reference	Adopted O/I method	Aquifer Type	Location	Factors of verifying vulnerability map	Key findings
Lobo Ferreira et al. (2005)	GALDIT	UCA [a]	Monte Gordo, Portugal	-	● Hazards due to climate change (i.e. SLR) and overexploitation of aquifer have significant impacts on vulnerability of coastal aquifer due to SWI.
Kallioras et al. (2011)	GALDIT, Pesticide DRASTIC	UCA	Xilagani, northern Greece	Cl^-, NO_3^-, and ratio of $Cl^-/[HCO_3^- + CO_3^-]$	● Modifications on weighting factors of DRASTIC and GALDIT are necessary. ● Both DRASTIC and GALDIT have acceptable coincide with the chemical indicators.
Mahesha et al. (2012)	GALDIT	UCA	West of India	Ratio of Cl^-/HCO_3^-	● GALDIT method for vulnerability assessment of coastal aquifers to SWI due to projected sea level rise is a quite effective and reasonable.
Najib et al. (2016)	GALDIT	UCA	Northwest of Morocco	Pumping rate	● The obtained vulnerability map has acceptable coincide with the pumping rate.
Saidi et al. (2013)	GALDIT, AVI [b]	UCA	Mahdia-Knsour Essaf, Tunisia	Simpson's ratio [e], ratio of SO_4^{2-}/Cl^-, ratio of Cl^-/Br^-, and NO_3^-	● Both GALDIT and AVI capable to produce vulnerability maps that are significantly correlated with the verifying factors. ● The biggest limitation associated with these methods is spatial interpolation of observed point data over across the aquifer.
Sophiya and Syed (2013)	GALDIT	UCA	Ramanathapuram, eastern India	Cl^-	● Temporal variations of influenced parameters (e.g. hydraulic conductivity, recharge rate, and distance from coast) on SWI in the spatial pattern over the aquifer is necessary.
Kura et al. (2014)	GALDIT, DRASTIC	UCA	Kapas, northeast Malaysia	NO_3^-	● Very strong negative correlation between GALDIT and groundwater resistivity is observed (r=−0.86), whereas DRASTIC model is more correlated to NO_3^- data (r=0.56).
Tamaszkiewicz et al. (2014)	GQI_{SWI}	UCA	15 worldwide coastal aquifers	f_{sea}, EC, TDS, and SAR [d]	● SWI entails complex Hydrogeochemical process that cannot be fully captured through the GQI_{SWI}. ● GQI_{SWI} can be used for preliminary assessments.
Pedreira et al. (2015)	GALDIT, Pesticide DRASTIC	UCA	Northeastern Greece	Cl^- and NO_3^-	● The parameter height of groundwater table above sea level is a very significant factor for evaluating the vulnerability of aquifer to SWI.
Recinos et al. (2015)	GALDIT	UCA	Northern Greece	Cl^-	● Height of groundwater above sea level (L) and impact magnitude of existing SWI (I) are the critical parameters on vulnerability of aquifer due to SWI.
Bouderbala et al. (2016)	GALDIT, AVI	UCA	Nador, northern Algeria	WQI [h]	● GALDIT doesn't included the anthropogenic effect of pumping wells. ● Both methods are efficient tools to show the effect of SWI and have acceptable coincide with WQI.
Docheshmeh-Gorji and Asghari-Moghadam (2016)	GALDIT, AHP-GAPDIT [i]	UCA	Azarshahr, northeast of Iran	TDS	● Pumping rate (parameter P) has higher impact on aquifer vulnerability due to SWI than groundwater table above sea level (parameter L). ● Pumping rate can be used for parameter L in case of scarcity of observation wells.
Trabelsi et al. (2016)	GALDIT, GQI_{SWI}	UCA	Northern Sfax basin, Tunisia	Jones ratio [c], Cl^-, and TDS	● Vulnerability map produced by the GALDIT is more convincing. ● GQI_{SWI} can be served as complementary method to verifying the GALDIT map. ● Superiority of GALDIT method is due to involving the hydro-dynamic condition of aquifer (e.g. permeability and groundwater level)
Klassen and Allen (2017)	CVM [j]	UCA	British Columbia, Canada	EC	● Hazards due to pumping have the greatest influence on the coastal aquifer vulnerability due to SWI.

					● Use of chemical indicators of groundwater is essential for accurate identifying of vulnerable areas to SWI.
Luoma et al. (2017)	AVI, SINTACS [k], GALDIT	UCA	Southern Finland	f_{sea}, and length of SWI wedge estimated by Ghyben-Herzberg Eq.	● GALDIT and then SINTACS provide better insight into groundwater vulnerability to SWI in aquifers with low hydraulic gradient and ones strongly impacted by recharge rate and SLR due to climate change. ● AVI and then SINTACS provide better vulnerability mapping to anthropogenic source on the ground surface. ● Groundwater level is the most influential factor in groundwater vulnerability of coastal aquifers. ● Drawbacks of I/O methods are use of qualitative parameters, large amount of data required (especially GALDIT and SINTACS), and a few vulnerability discretization.
Allouche et al. (2017)	DRASTIC, GALDIT	UCA	Northern Sfax basin, Tunisia	NO_3^- and groundwater resistivity	● Adding land use parameters to both methods lead to obtain a reliable vulnerability map. ● Significant negative correlation was observed between the GALDIT and groundwater resistivity (r = -0.61).
Metevalli et al. (2018)	Modified GALDIT and TAWLBIC [g]	CA/UCA/LA	Ghaemshahr-juybar, northern Iran	EC, TDS, and SAR	● Necessity of identifying the influential factors on SWI to produce vulnerability map through O/I methods, especially in coastal aquifers influenced by both inherent susceptibility and anthropogenic factors (e.g. pumping) in SWI process. ● High correlation is obtained between the mapped output of combined GALDIT and TAWLBIC (averaged r= 0.73) and Hydrogeochemical indicative factors in comparison with individual models (averaged r= 0.63 and 0.68, respectively). ● Depth to groundwater and groundwater level decline is the most important factors in GALDIT and TAWLBIC, respectively.
Kazakis et al. (2018)	GALDIT-F (GALDIT coupled with fuzzy multi-criteria categorization)	CA/UCA	Northern Greece	Cl^-, and ER[f]	● One of drawbacks of typical GALDIT is limited discretization of vulnerability scores. ● GALDIT-F produces a higher discretization of vulnerability scores to SWI. ● Testing the robustness and verification of vulnerability degree produced by the O/I methods through indicative pollutants concentration in groundwater is a main challenge.

[a] UCA, CA, and LCA denotes to unconfined, confined, and leaky aquifer, respectively. [b] AVI uses two key parameters including thickness of each sedimentary unit above the uppermost aquifer, and estimated hydraulic conductivity of each of these layers . [c] Jones ratio is defined as Na^+/Cl^-. [d] SAR is sodium adsorption ration. [e] Simpson's ratio is defined as $Cl^-/(CO_3^{2-} + HCO_3^-)$. [f] ER denotes to electrical resistivity tomography of aquifer. [g] TAWLBIC denotes to salt-water up-coning vulnerability indices. [h] Water Quality Index which calculated by $WQI = \sum_{i=1}^{n} W_i \times (C_i/S_i)$, where W_i is relative weight of i^{th} chemical parameter, C_i is concentration of i^{th} chemical parameter, and S_i is World Health Organization (WHO) standard for i^{th} chemical parameter in groundwater. [i] AHP denotes to Analytic Hierarchy Process, and GAPDIT is GALDIT method in which groundwater table above sea level (parameter L) is replaced by the pumping rate (parameter P). [j] CVM denotes to Combined Vulnerability Model which considered the effects of climate change-related hazards (SLR and storm surge), an anthropogenic hazard (pumping), and aquifer susceptibility hazards (distance from coast and topographic slope). [k] the acronym SINTACS originates from the initials (in Italian) of seven factors ''Soggiacenza'' as depth to water, ''Infiltrazione'' as net recharge, ''Non saturo'' as impact of vadose zone, ''Tipologia di copertura'' as soil media, ''caratteristiche dell' Acquifero'' as aquifer media, ''Conduciblita idraulica'' as hydraulic onductivity, ''acclivita di superficie topografica (S)'' as slope.

Table 2. GALDIT parameter weights, rates, and ranges (Chachadi and Lobo-Ferreira 2001)

Rating	Groundwater occurrence (aquifer type) G (-)	Aquifer hydraulic conductivity, A (m/day)	Height of groundwater level above sea level, L (m)	Distance from the shore line, D (m)	Impact of the existing status of seawater intrusion, I			Aquifer saturated thickness, T (m)
					$Cl^-/[HCO_3^- + CO_3^{2-}]$[b]	EC ($\mu S/cm$)	Cl^- (mg/l)	
10 (High)	Confined aquifer	>40	<1	<500	>2	>1000	>200	>10
7.5 (Medium)	Unconfined aquifer	10-40	1-1.5	500-700	1.5-2	800-1000	100-200	7.5-10
5 (Low)	Leaky confined aquifer	5-10	1.5-2	700-1000	1-1.5	400-800	25-100	5-7.5
2.5 (Very Low)	Bounded aquifer[a]	<5	>2	>1000	<1	<400	<25	<5
Weight	1	3	4	4	1	1	1	2

[a] An aquifer that the recharge and/or impervious boundary, aligned parallel to the coast.

[b] The ions have unit of meq/l.

Table 3. Vulnerability rating and weighting adopted for the parameter i in GAiDIT and GALDIT-i methods

Rating	Seaward hydraulic gradient of freshwater, i (m/m)
10 (High)	< 0.2
7.5 (Medium)	0.2-0.4
5 (Low)	0.4-0.6
2.5 (Very Low)	> 0.6
Weight	4

Table. 4. Hydrogeology characteristics of three studied aquifers (GRWA 2015).

Aquifer Name	Aquifer Type	N_{piez} $(-)$	$A\ (km^2)$	$\Delta h\ (m)$	ΔV (MCM)	$S_c\ (-)$	$T\ (m^2/d)$	$\bar{P}\ (mm)$	$GW_D\ (m)$	$GW_L\ (m)$	$B\ (m)$
Fomanat	Confined	73	1809.5	-0.04	-1.91	0.02* 0.51 1.20	100 570 3000	1046.7	0.65 2.85 18.68	-26.0 -10.0 95.0	14.5 40.0 80.0
As-Ko	Confined/ Phreatic	80	783.0 /206.5	-0.04	-0.82	0.001 0.027 0.098	600 1945 4000	1430.0	1.0 2.4 4.0	-27.0 -10.1 40.0	10 44.5 92
La-Ch	Phreatic/ Confined	95	847.0	-0.1	-2.43	0.00007 0.0018 0.0083	21 467 1384	1228.0	0.95 2.45 13.5	-26 -3.5 55	7.0 31.0 76.0

N_{piez} is number of piezometers to monitor the groundwater level, A is area of aquifer plain, Δh is average annual variation of groundwater level during 1992-2013, ΔV is average annual variation of groundwater storage, S_c is storage coefficient of aquifer, T is transmissivity of aquifer, $\bar{P}$ is average annual rainfall on the aquifer plain, GW_D is the depth to groundwater, GW_L is groundwater level above mean sea level (MSL), B is thickness of aquifer (saturated part), EC is electrical conductivity of groundwater, Cl^- is the concentration of chloride ion in groundwater based on the newest available data (year 2013).

* Denotes to minimum, average, and maximum values, respectively.

Table 5. Average value of the parameters adopted in SWI vulnerability mapping across three aquifers based on latest available hydrogeological data (year 2013).

Parameter (unit)	As-Ko	Fomanat	La-Ch
$A\ (km^2)$	2303.0	2027.3	854.0
$z_0\ (m)$	99.27	202.93	54.54
$h_0\ (m)$	81.0	94.0	86.0
$h_f\ (m)$	22.76±17.60*	40.44±26.32	23.0±17.46
$\rho_s\ (kg/m^3)$	1008.20	1008.20	1008.20
$K\ (m/d)$	18.60	6.40	4.89
$q'\ (m^2/d)$	0.085±0.012	0.043±0.003	0.056±0.002
W_{net} ** (mm/d)	3.15	3.13	2.41
$L_T\ (m)$	637.3±58.86	371.4±43.92	328.4±26.47

* Standard deviation of monthly data for the parameter

** Estimated through the groundwater balance by GWRA

Table 6. Results of GALDIT, GAiDIT, and GALDIT-i vulnerability index in specified vulnerability classification.

Vulnerability Class	Aquifer	GALDIT		GAiDIT		GALDIT-i	
		Area (km^2)	Area (%)	Area (km^2)	Area (%)	Area (km^2)	Area (%)
Low	La-Ch	801.9	93.9	75.5	8.8	144.6	10.9
	As-Ko	1807.9	78.4	452.7	19.7	6.9	0.3
	Fomanat	1788.1	88.2	266.2	9.5	654.8	32.3
Moderate	La-Ch	52.1	6.1	282.5	33.1	337.6	39.5
	As-Ko	495.1	21.4	723.0	31.4	1149.2	49.9
	Fomanat	239.2	11.8	790.4	35.4	748.1	36.9
High	La-Ch	0.0	0.0	496.0	58.1	371.8	49.5
	As-Ko	0.0	0.0	1127.4	49.0	1146.9	49.8
	Fomanat	0.0	0.0	970.7	44.3	624.4	30.8

Table 7. Pearson's correlation coefficient (PCC) between the vulnerability index values produced by three GALDIT, GAiDIT, and GALDIT-i models and observed concentrations of TDS, indexes of f_{sea} and $\overline{GQI}$, and estimated values of L_x in three studied aquifers*.

Vulnerability Index	Aquifer	TDS (mg/l)	f_{sea} (-)	$\overline{GQI}$ (-)	L_x (m)	Average
GALDIT	As-Ko	0.323	0.327	0.356	0.463	0.367
	Fomanat	0.263	0.248	0.473	0.291	0.319
	La-Ch	0.493	0.403	0.431	0.263	0.398
GAiDIT	As-Ko	0.424	0.416	0.450	0.445	0.440
	Fomanat	0.749	0.718	0.753	0.244	0.616
	La-Ch	0.696	0.746	0.694	0.394	0.633
GALDIT-i	As-Ko	0.526	0.529	0.570	0.549	0.544
	Fomanat	0.859	0.821	0.733	0.485	0.725
	La-Ch	0.756	0.798	0.754	0.522	0.708

* All correlation coefficients are significant at α=0.05.

Table 8. The percentage of variation (PV) in the GALDIT and GAiDIT vulnerability indexes respect to 10% of increasing in the scores of incorporated indicators adopted for three studied aquifers.

Indicator	La-Ch Aquifer			Fomanat Aquifer			AS-Ko Aquifer		
	GALDIT	GAiDIT	GALDIT-i	GALDIT	GAiDIT	GALDIT-i	GALDIT	GAiDIT	GALDIT-i
G*	1.40	1.09	1.06	1.38	1.05	1.04	1.15	0.85	0.84
A	2.02	1.84	1.53	2.45	2.11	1.83	2.02	1.71	1.48
L	2.41	-	1.83	2.56	-	1.92	3.00	-	2.19
i	_	2.86	2.38	_	2.85	2.48	_	3.11	2.69
D	0.81	0.73	0.62	0.71	0.57	0.53	0.98	0.83	0.72
I	2.22	2.20	1.69	1.69	2.20	1.27	1.87	2.54	1.37
T	1.19	1.27	0.90	1.22	1.19	0.92	1.01	0.97	0.74

* The percentage of variation for indicator G is obtained by changing the aquifer type from confined to unconfined.